Norwegian University of Life Sciences
Faculty of Vetrinary Medicine and Bioscience
Department of Chemistry, Biotechnology and
Food Science

Master Thesis 2015
60 credits

Investigating Novel Biomarkers for Neonatal Asphyxia in Newborn Piglets

Sophia Manueldas

Acknowledgements

The work presented in this master thesis was carried out in the Pediatric research (PFI) group of Ola Didrik Saugestad, at Oslo University hospital from August 2014 to May 2015. This scientific thesis represents the completion of the academic degree of Civil Engineer (Master of Science) in Chemistry and Biotechnology.

First of all, I want to thank my supervisor Dr. Lars O. Baumbusch for giving me the opportunity to write my thesis in collaboration with the pediatric research group. You have given me excellent supervision, motivation and scientific guidance. You have always taken time and had faith in me. I am grateful for all the constructive feedback and help during the writing process. I have learned a lot from you, which I will always be thankful for. I would also thank my internal supervisor Tor Erling Lea for continuous guidance.

Thanks to Torkil Benterud for endless optimism, advice and support. Especially for all the help with writing process and statistic. I want to thank Monica Åsegg-Atneosen for always being positive. I am grateful for all your help with lab technical issues, and for giving valuable advice and motivation. Also big thanks to Grethe Dyrhaug, for always have being supportive at the lab. Thanks to Professor Ola Didrik Saugestad to letting me write my thesis at your department -an experience I will always remember. I also want to thank all the members of PFI for supporting me through this work. It was a pleasure to work with all of you.

Last but not least, thanks to my greatest family, friends and love ones for all your support, encouragement, motivation and care throughout the process. Special thanks to my parents and Dhanushan, you always gave me the support and understanding I needed to finish my degree.

Sophia Manueldas

Oslo, May 2015

Abstract

Perinatal asphyxia is a condition in neonates with reduced oxygen (hypoxia) and/or reduced perfusion (ischemia). Today, we lack good biomarkers to measure the degree of oxidative damage caused by perinatal asphyxia. This thesis is about to testing and establishing two potential biomarkers for perinatal asphyxia: (a) random mutation capture assay (RMC) and (b) cell-free DNA (cfDNA). RMC is based on single molecule amplification and restriction digest to detect mitochondrial and nuclear mutations. Increased amount of cfDNA in circulating blood is found in patients with cancer, stroke and in premature infants.

The reaction spectrum of RMCs potential was tested by treating a fetale pig cell line, EFN-R, with different concentrations of H_2O_2 over different time intervals. The oxidative damage was monitored by RMC, in both the mitochondrial DNA (12S) and nuclear DNA (p53 gene). We observed an increased degree of DNA damage by oxidative stress substantially greater in nuclear DNA compared to mitochondrial DNA. Furthermore, antioxidant N-acetylcysteine amide (NACA) was investigated and identified as a significant protective agent against oxidative damages. To study the damage on expression level, RNA expression studies were performed for *p53*, *Bax* and *Caspase 3* followed by protein expression studies for BAX.

To investigate cfDNA as biomarker for oxidative damage 80 newborn pigs, a model system very close to the human, were exposed to hypoxia and reoxygenation. A group of pigs was further treated with either NACA or hypothermia. Various extraction methods and standard curves for isolating cfDNA were tested and the concentration of cfDNA was measured by photometric and qRT-PCR methods (β-globulin). The concentration of cfDNA was highest 30 minutes after reoxygenation of hypoxia. The same tendency was observed by the photometric and qRT-PCR methods. However, no statistical significance was found. The thesis concludes that both RMC and cfDNA may be used as non-invasive biomarkers for assessing the degree of oxidative damage in newborns for perinatal asphyxia.

Sammendrag

Perinatal asfyksi er en tilstand hos nyfødte barn med redusert oksygen (hypoxi) og/eller redusert perfusjon (iskemi). I dag mangler vi gode biomarkører for å måle graden av oksidativ skade ved perinatal asphyxi. Denne oppgaven handler om å teste og etablere to potensielle biomarkører for perinatal asfyksi: (a) random mutation capture assay (RMC) og (b) cellefritt DNA (cfDNA). RMC er basert på singel-molekyl amplifikasjon og restriksjonskutting for å detektere mitokondrielle og nukleære mutasjoner. Økt mengde av cfDNA i sirkulerende blod ble funnet i pasienter med kreft, slag og hos premature barn.

Reaksjonsspektrum av RMCs potensial ble testet ved å behandle fetale EFN-R grisecelle linje med ulike konsentrasjoner over forskjellige tidsintervaller med H_2O_2. Oksidative skader ble monitorert ved RMC i både mitokondriell DNA (12S) og nuklære DNA (p53). Det ble observert en økt grad av DNA skade ved oksidativ stress, og skadene er betydelig større i nukleær DNA sammenlignet med mitokondriell DNA. Videre ble det undersøkt om antioksidanten N-acetylcystein-amid (NACA) virker protektiv ved oksidativ skade. Det viste seg at NACA har en signifikant effekt som protektiv agens. For å studere skadene på ekspresjonsnivå ble det gjort RNA ekspresjonstest med genene *p53*, *Bax* og *Caspase 3* og protein ekspresjonsstudier med proteinet BAX.

For å teste cfDNA som biomarkør for oksidativ skade, ble 80 nyfødte griser, et modellsystem svært nært det humane, eksponert for hypoxi og reoksygenering. En gruppe gris ble videre behandlet med enten NACA eller hypothermi. Under forløpet ble ulike ekstraksjonsmetoder og standardkurver for isolering av cfDNA ekstrahert og konsentrasjonen av cfDNA ble målt med fotometrisk eller qRT-PCR metoder (β-globulin). Konsentrasjonen av cfDNA er vist å være høyest 30 minutter etter reoksygenering ved hypoxi. Til tross for at samme tendens observeres ved både qRT-PCR og fotometrisk metode, påvises ingen statistisk signifikans. Oppgaven konkluderer med at både RMC og cfDNA vil kunne anvendes som non-invasive biomarkører for å vurdere graden av oksidative skader hos nyfødte ved perinatal asfyksi.

Table of contents

Abbreviations

ATP	Adenosine triphosphate
Bcl-2	B-cell lymphoma 2
BE	Base Excess
BER	Base excision repair
bp	base pair
cDNA	Copi DNA
cfDNA	Cell free DNA
ct	Cycle threshold
dNTP	Deoxynucleotide
HI	Hypoxia-Ischemia
mtDNA	Mitochondrie DNA
NAC	N-acetylcysteine
NACA	N-acetylcysteine amide
NADPH	Nicotinamide adenine dinucleotide phosphate-oxidase
ntDNA	Nuclear DNA
OD	Optical density
PCR	Polymerase Chain reaction
qRT-PCR	Quantitative real-time PCR
RMC	Randome mutation capture
ROS	Reactive oxidative species
rpm	Revolutions per minute
SDS-PAGE	Sodium dodecyl sulphate polyacrylamode gel electrophoresis
WT	Wild-type
ETC	Electron transport chain
GSH	Glutathione
MTT	3,4,5 dimethylthiazol-2,5 diphenyl tetrazolium

1.0 Introduction

1.1 Asphyxia

1.1.1 Birth asphyxia

Every year, 6.6 million children under five years die worldwide mainly due to infectious, pre-term birth complications, and birth asphyxia (also called neonatal or perinatal asphyxia) [1, 2]. Asphyxia is a term comprehending different forms of reduced oxygen flux, leading to impaired or absent oxygenation of tissue [3, 4]. In the context of perinatal mortality, the lack of oxygen strikes mainly the brain, frequently leading to cerebral palsy [5]. In 2010, it has been estimated that of the 800 000 children facing birth asphyxia per year, 40 000 will develop cerebral palsy [2].

In the clinic, a common definition of birth asphyxia is generally accepted and in use [3, 6], embracing four aspects of childhood health: (1) metabolic academia (pH<7.00) in the arteria umbilicalis, (2) an Apgar score (describing the physical condition of a newborn) of below 4 after 5 minutes, (3) neonatal neurologic complications, and (4) effectiveness to several organs.

Several reasons for perinatal asphyxia exist, including hypo- and hypertension, retained placenta (the placenta only partially separates from the uterus), decreased concentration of oxygen in mother's blood before and during birth, and infectious diseases. Postnatal causes to asphyxia are typically associated with malformation or occlusion in the respiratory tract [7, 8]. Intervention strategies are limited, and there is still a lack of reliable diagnostic biomarkers for prediction of the severity and outcome after neonatal asphyxia.

1.1.2 Perinatal hypoxia – ischemia (HI)

Birth asphyxia is a condition of hypoxia (lack of oxygen), metabolic acidosis (increased acid levels), and ischemia (reduced blood perfusion). Hypoxia together with acidosis compromises myocardial function, resulting in hypotension, decreased blood flow, and ischemia in organs and tissues [4, 9]. The combination of reduced arterial O_2-

concentration together with non-sufficient blood flow is called hypoxia-Ischemia (HI) [3]. Global HI-injury in the developing brain can result from a variety of clinical conditions [10]. HI may damage various vital organs of the infant, including the heart, lungs, kidneys, and the central nervous system (brain). Damages to the brain are of major concern, since they lead to life long lasting neurological complications and there is a demand to minimize the brain damage triggered by the event of asphyxia [11].

1.1.3 Phases of HI-related brain damage and intervention strategies

The first phase of brain damage results in early cell death, mostly a result of severe hypoxia. Brain injury caused in the first phase will occur within few minutes. However, immediate resuscitation to restore oxygen supply and blood circulation may limit the damage [10, 12].

A secondary phase injury occurs 6-48 hours after the initial insult. Free radical production, intracellular calcium entry, and apoptosis are three important mechanisms [13]. Treatments during the post-resuscitation phase can block these processes and limit the secondary cell damage and minimize the extent of brain damage. Global HI triggers several cellular and biochemical pathways, which can result in secondary neuronal injury after reoxygenitation **(figure 1.1).** One crucial mechanisms of secondary neuronal injury after global HI is inflammation [10, 14].

Several mechanisms are related to immediate effects of energy failure. This can result in decreased production of energy-rich phosphate compounds. The effect of energy failure is often related to functional reduction of pre-existing proteins. However, when oxygen is re-established a secondary energy failure can be alterations of gene expression, cell survival, and neurogenesis [3].

Latent phase follows reoxygenation. In this phase, a so-called therapeutic window is available for potential neuroprotective intervention. Basically, the only clinically used treatment with significant effect is hypothermia [5]. Hypothermia is achieved by cooling the infant, until a body temperature of 33°C is reached [15]. Studies have shown that neonates treated with hypothermia, has a significantly better neurologic outcome

compared to infants not treated by hypothermia [10]. A reduction in mortality is also documented [10, 16]. However, the positive effects are only to a certain extent. Thus, developing alternative treatments in addition to hypothermia is desirable.

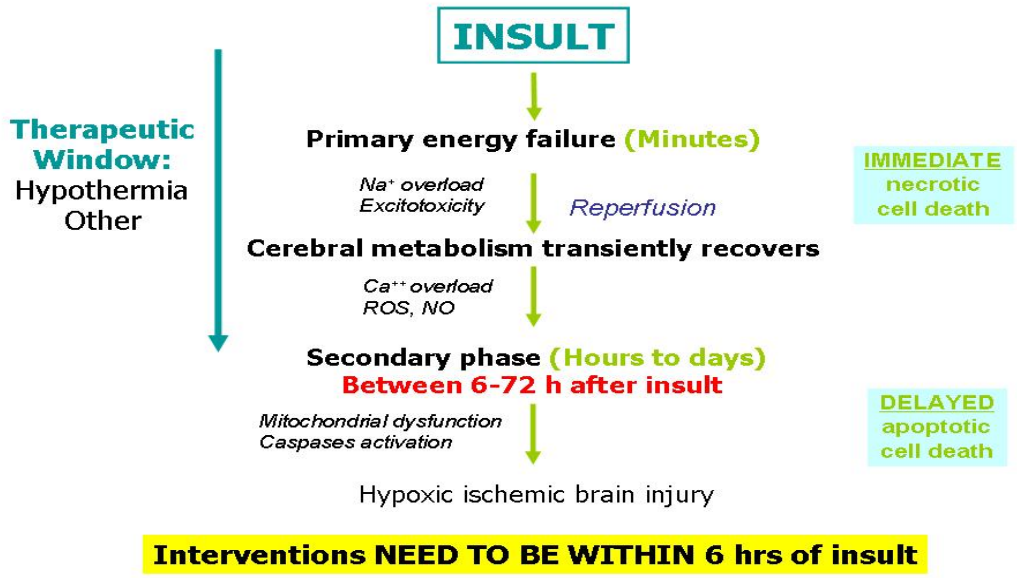

Figure 1.1: Schematic representation of global HI and following phases. First phase involves primary energy failure. This will occur immediately. Followed by a secondary phase. This will occur several hours after insult. In this stage a therapeutic window is available, where we can treat the incidence with hypothermia [17].

1.1.4 Animal models

Studying the pathogenesis of neonatal asphyxia in human is difficult. Therefore pigs and other experimental animals have been used as model organisms. Because of the anatomical and physiological similarities, pigs have been preferred as animal model for biomedical research [18]. In addition, the embryologic development of the brain is similar. In the piglet brain growth and myelinization, brain maturation, and distribution of grey to white matter are all comparable to the newborn human brain [19, 20]. Pigs have also similarities to human development at pregnancy in week 36-38.

1.2 Oxidative stress and reactive oxygen species (ROS)

All aerobic organisms are dependent on oxygen for efficient energy production [21]. These oxygen molecules catalyze other molecule with high chemical reactivity leading to formation of reactive oxygen species (ROS), which are potentially harmful to the organism. ROS are formed as natural by-products of the normal metabolism of oxygen. This event has an important role in cell signaling and homeostasis [22].

ROS is a general term for oxygen radicals (free radicals) with great potential to exchange electrons with other molecules. It includes superoxide ($*O_2^-$) and hydroxyl radical (*OH), as well as non-radical compounds such as hypochlorous acid (HOCl) and hydrogen peroxide (H_2O_2) [23]. At physiological levels, ROS are useful as effector molecules in the immune system for phagocytic clearance of microorganisms and for mediators for signal transduction and gene expression [24].

During environmental stress, ROS levels increase dramatically. This results in significant damage to cell structures. Elevated levels of ROS can damage many components and macromolecules of the cell. These include proteins, lipids, carbohydrates, and DNA. DNA damage stimulate mutation and lead to aging as well as inheritable diseases and cancer [23]. ROS also induce carbonylation of proteins and alter the function of biologic important proteins [25]. Peroxidation of membrane lipids results in cell damage through disruption of cellular membranes. ROS can cause non–enzymatic degradation of glycosaminoglycan leading to the decreased viscosity of fluids and tumor [26].

As described above free radicals that are produced by ROS lead to chain reactions and cause damage or death to the cell. Antioxidants terminate these chain reactions and help to reduce the level of ROS by (1) preventing the formation, (2) removing already formed ROS – called scavengers, or (3) repairing already damaged molecules [23, 27].

Normal cellular antioxidant defense mechanisms include enzymatic and non-enzymatic antioxidants [28]. Enzymatic antioxidants include catalase, superoxide dismutase (SOD), glutathione peroxidases (GP_x), glutathione-S-transferase (GST) and glutathione reductase (GR). The non-enzymatic antioxidants are glutathione (GSH) and protein

thiols [24]. The antioxidants balance the low and moderate levels of ROS to maintain the redox equilibrium of a cell **(figure 1.2)** [29].

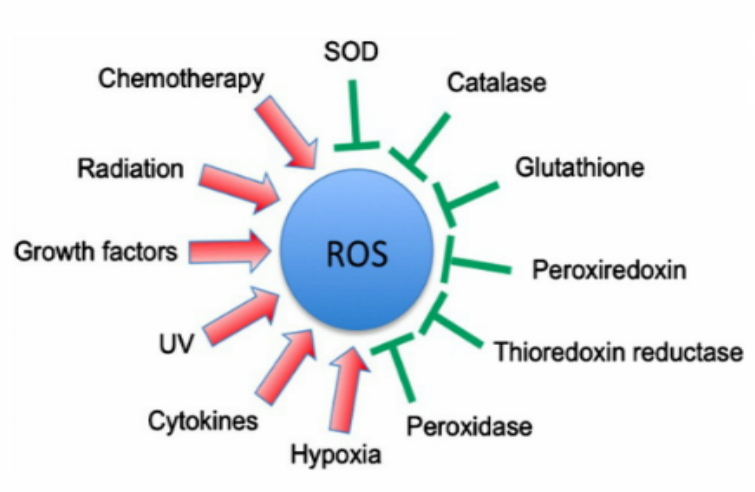

Figure 1.2: Representation of different activators and inhibitors for production of reactive oxygen species [30].

Both systemic and local hypoxia may cause oxidative stress. In tumors, for instance, the high degree of cell proliferation increases the need of oxygen, and causes a local hypoxia [31]. Systemic and local hypoxia triggers the same reaction; lipid peroxidation, protein modifications, DNA damage, mitochondrial dysfunction, and genes like hypoxia-inducible factor-1 (*HIF-1*), *Caspase*, NF-KappaB (*NF-$_k$B*), *GAFP, Bax* and *p53* **(figure 1.3)** [10].

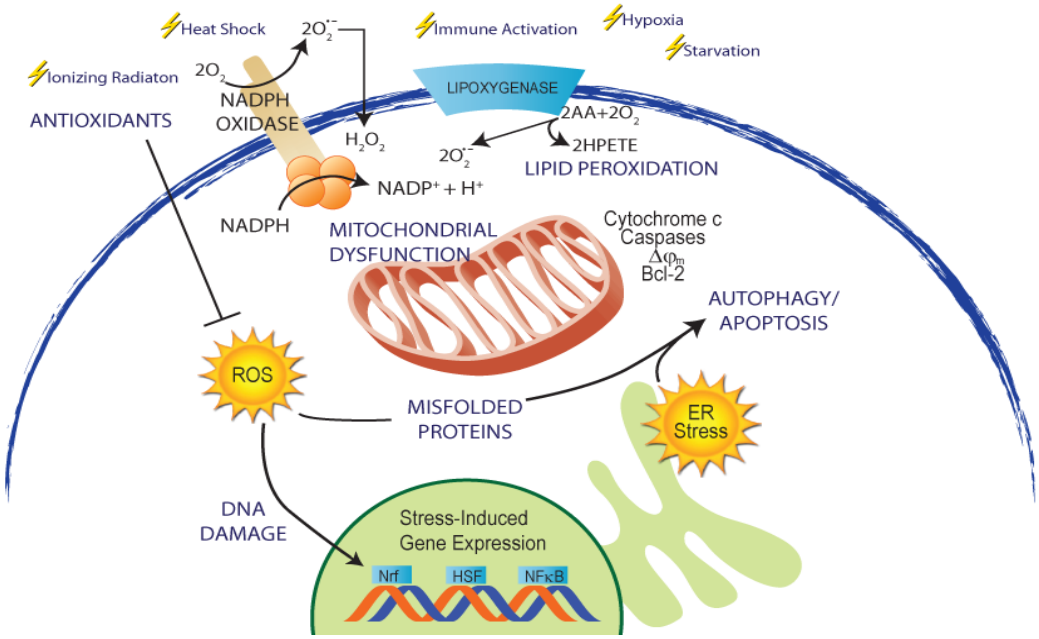

Figure 1.3: Systemic and local hypoxia triggers the same reactions (lipid peroxidation, protein modifications, DNA damage and mitochondrial dysfunction) and genes (including *HIF-1, caspase, NF$_k$B, GAFP, Bax,* and *p53*) [32].

1.3 Biomarkers for oxidative stress and DNA damage

Measuring oxidative stress and oxidative damage to DNA and proteins non-invasively in asphyxiated newborns could be a tempting method to investigate grade of damage [3]. Biomarkers are defined as "characteristics that can be objectively measured and evaluated as indicators of normal biological processes, pathogenic processes, or pharmacologic responses to a therapeutic intervention" [33]. Many biomarkers are used as parameters to measure oxidative stress damage, for instance ROS levels, NADPH oxidase activity assay, GSH/GSSG, antioxidant enzyme activity assay, and ATP levels **(figure 1.3)** [34]. Various biomarkers for oxidative stress are available. Different biomarkers for DNA damage have been developed in the last decades. Instance oxidized bases in DNA can be measured directly by high-performance liquid chromatography (HPLC) and comet assay can be used to detect the DNA breaks.

Although most of the marker have limited value in vivo because they lack sensitivity and/or specificity or require invasive methods [33]. However, there is still a demand for a reliable method for measuring oxidative stress caused by neonatal asphyxia.

1.3.1 DNA damage

Main sources of oxidative DNA damage are ROS (see 1.2). DNA damaging agents may induce various modifications to DNA. A cell can form more than 20 000 DNA lesions per day from endogenous sources. These lesions are mainly non-bulky and arise mostly through endogenous sources [35, 36].

Several pathways have been developed by organism to repair DNA. In addition, different checkpoints in DNA damage are established to resist the challenge of endogenous and exogenous DNA insults. DNA insults are results from either cellular metabolic processes (endogenous sources) or environmental factors (exogenous sources). Hydrolysis, oxidation, alkylation, crosslinking, and mismatch of DNA are all endogenous sources for DNA damage.

Sources for exogenous DNA damage include ionizing radiation (IR), ultraviolet (UV) radiation, and various chemical agents [35, 37, 38]. Ionizing radiation give rise to DNA strand breaks and may induce production of ROS (see 1.2). DNA damages that is not properly repaired at cellular level and DNA which is modified, can lead to genomic instability, changes in gene expression, apoptosis, or senescence (**figure 1.4**). Causes like loss of genomic integrity can lead the organisms to neurological disorders, cancer and immunodeficiency. This may affect the development of the organism and the aging process [35, 37].

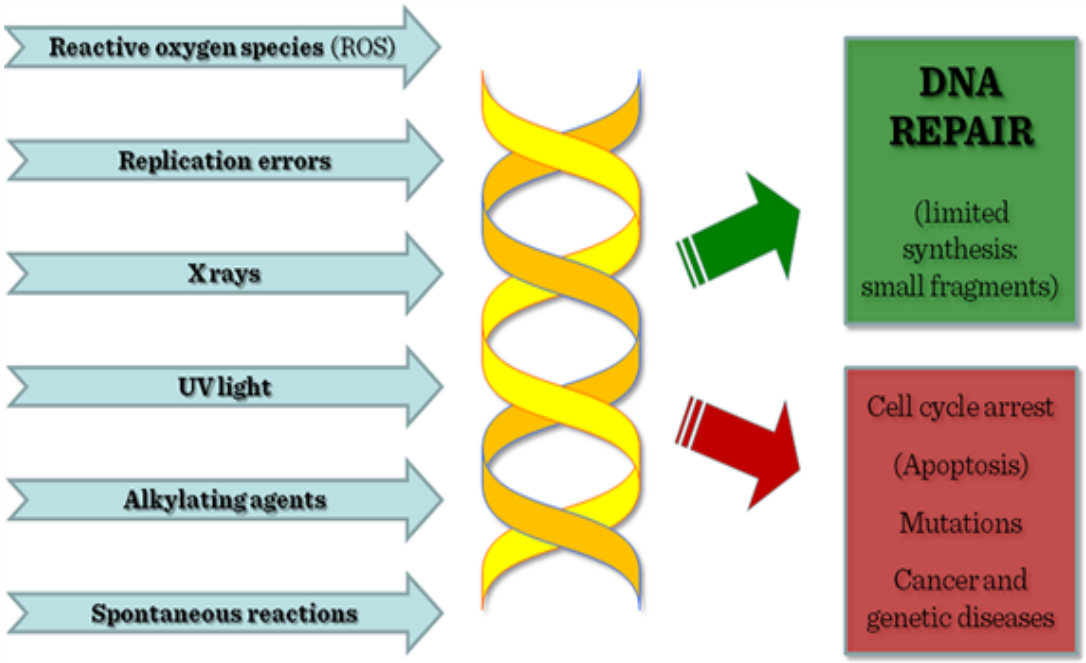

Figure 1.4: ROS, X-ray, UV light are one of several causes of DNA damage. After a DNA damage insult, different outcome are possible; DNA repair or cell cycle arrest, mutations, cancer and diseases [39].

DNA damage in organs is the cause of different diseases like Alzheimer and Parkinson [40, 41]. Nevertheless, the brain is the organ that has large consumption of oxygen, abundant lipid content, and regions with high level of iron, and relatively low amount of antioxidants. This makes the brain more vulnerable to oxidative stress compared to other organs [35, 42].

ROS-induced modifications of DNA include base lesions, modification on the ribose, and single- and double strand breaks. Specific repair systems for various DNA damage exists. Hence, the base excision repair (BER) is the primary pathway for the removal of base lesions from both nuclear DNA and mitochondrial DNA [43]. Although,

unrepaired base lesions can cause replication and transcription blockage, dependent on the lesion and the type of polymerase involved [44].

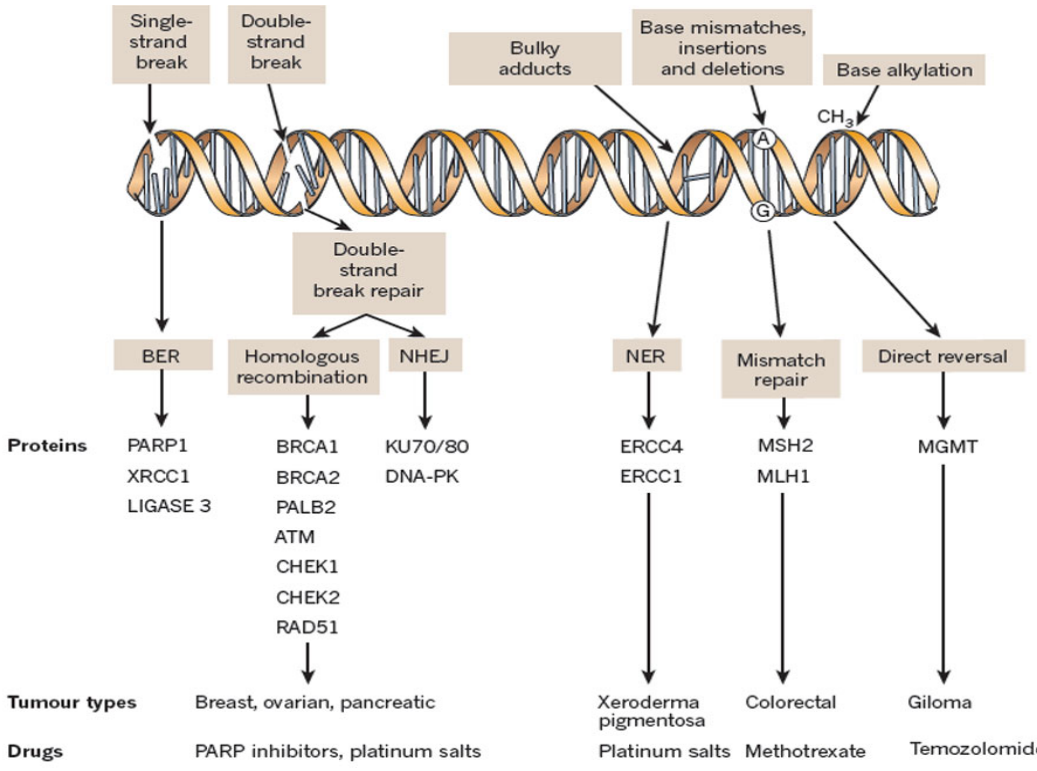

Figure 1.5: DNA damages as single strand breaks (SSB), double strand breaks (DSB), bulky adducts, mutations and alkylation with their representative repair mechanism, proteins, tumor types and drugs [45].

1.3.2 Mitochondrial DNA and nuclear DNA

Both, nuclear and mitochondrial genomes are continuously exposed to ROS derived from numerous endogenous and exogenous sources that induce oxidative damages to DNA [46]. Mitochondria are independent double membrane organelles (outer- and inner mitochondrial membrane) found in the cytosol of eukaryotic cells [47].

Similar to nuclear genome, the mitochondrial genome has double–stranded DNA that encodes for genes. The mitochondrial genome differs from the nuclear genome in several ways. The mitochondrial genome is circular and built of 16 500 DNA base pairs whereas the nuclear genome is linear and consists of 3.3 billion DNA base pairs [48].

The cell contains numerous mitochondria, and each mitochondrion contains 2-10 copies of the mitochondrial genome [49]. The mitochondrial genome is haploid in opposite to the nuclear genome, which is diploid and contains only 2 copies per cell. Moreover, the mitochondrial genome has a 10-times higher mutation rate than the nuclear genome [50, 51]. Potentially, increased level of aerobic metabolism can influence the different process, and therefore mitochondrial molecules are more vulnerable to oxidative damage [52, 53].

The generation of ROS is an unavoidable byproduct of electron transport chain (ETC) activity. Damage and mutation to mtDNA have a critical effect on ETC activity. The oxidative degradation of metabolites generates reducing equivalents that drive the ETC in the inner mitochondrial membrane. This ETC activity in the inner membrane is an important tool for cell signaling, apoptosis control, membrane potential and ATP production (**figure 1.6**) [52, 54, 55].

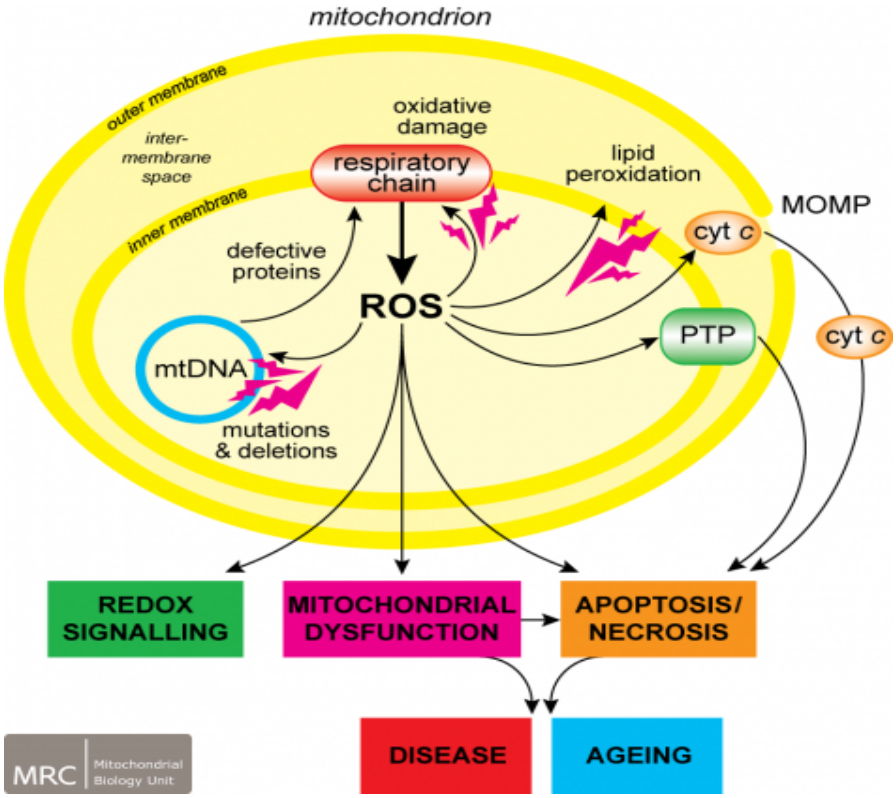

Figure 1.6: Overview of mitochondrial ROS production. Production of ROS by mitochondria can lead to oxidative damage to mitochondrial proteins, membranes and DNA. However, ROS can lead to redox signaling, mitochondrial dysfunction and apoptosis/necrosis. The latter can cause disease or ageing [56].

1.4 Genes expressed during oxidative stress

Both oxidative stress and ROS can damage the cells (see 1.2). Thus, ROS has been proposed a role as second messengers to regulate signal transduction pathways that ultimately control gen expression [57].

Gene expression is widely used as biomarker for different conditions. The gen expression from different genes can easily be measured by qRT-PCR. Oxidative stress can be regulated of several different genes, for instance *p53*, *Bax* and *Caspase 3*.

Activation of *p53* is triggered by several events like DNA damage, hypoxia, heat shock and various other stress signals (**figure 1.7**) [58-60]. *p53* is a human tumor suppressor protein encoded by the TP53 gene, which controls numerous signaling and cellular growth pathways [61]. *p53* wild type can activate DNA repair proteins when DNA has sustained damage [46]. When DNA damage has occurred, *p53* can arrest cell growth by holding the cell cycle at G1 regulation point. These allow the cell to repair the DNA damage, before further replication. However, if the DNA damage is too large to be repaired successfully, *p53* will trigger apoptosis by stimulating sensors that ultimately activate *Bax* [62].

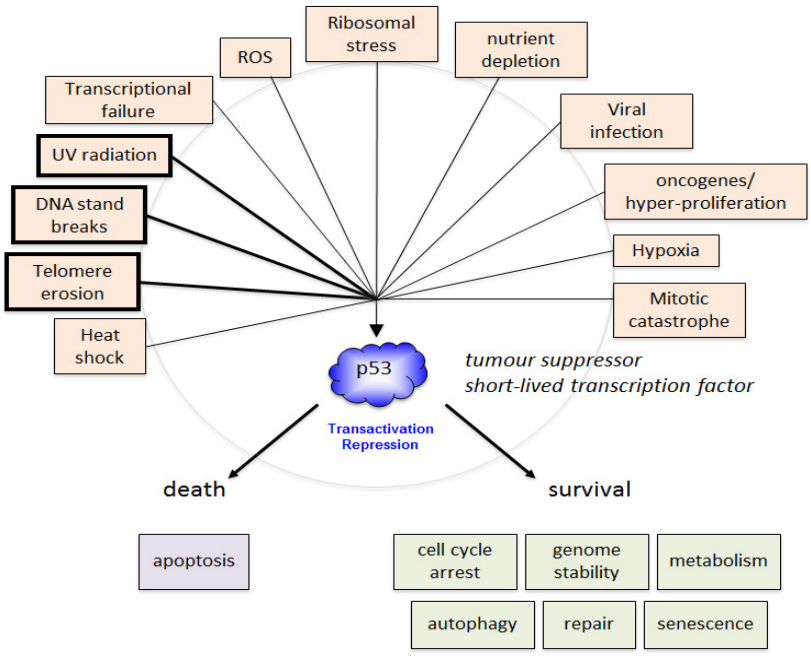

Figure 1.7: Factors as UV radiation, DNA strand breaks ROS that trigs p53 and result in either death or survival [63].

Bax is a pro-apoptotic bcl-2-family protein, which resides in the cytosol and translocates to mitochondria upon induction of apoptosis [64]. The permeability of the mitochondrial membrane is regulated by different protein in bcl-2 family. These proteins may be anti-(bcl-2) or pro-(Bax) apoptotic [65]. The regulation of threshold for apoptosis in the cells, has been suggested to be controlled by a balance between the pro-apoptotic and anti-apoptotic proteins [66].

Bax, which is an apoptotic trigger, leads to its translocation to the mitochondria and its subsequent insertion to mitochondria membrane. At the mitochondria, *Bax* can homodimerize or heterodimerize with other pro-apoptotic members [67]. It has been shown that *Bax* induce cytochrome c release and Caspase activation in vivo and vitro [68].

Caspase 3 is a member of the cysteine protease family, and may cleave bcl-2, not only inhibiting its anti-apoptotic effect, but also producing a pro-apoptotic fragment of bcl-2. The pro-apoptotic fragment will localizes to the mitochondrial membrane and causes the release of cytochrome c [65, 69]. Biochemically, the main features of apoptosis include Caspase cascade activation and DNA fragmentation [70] (**figure 1.8**).

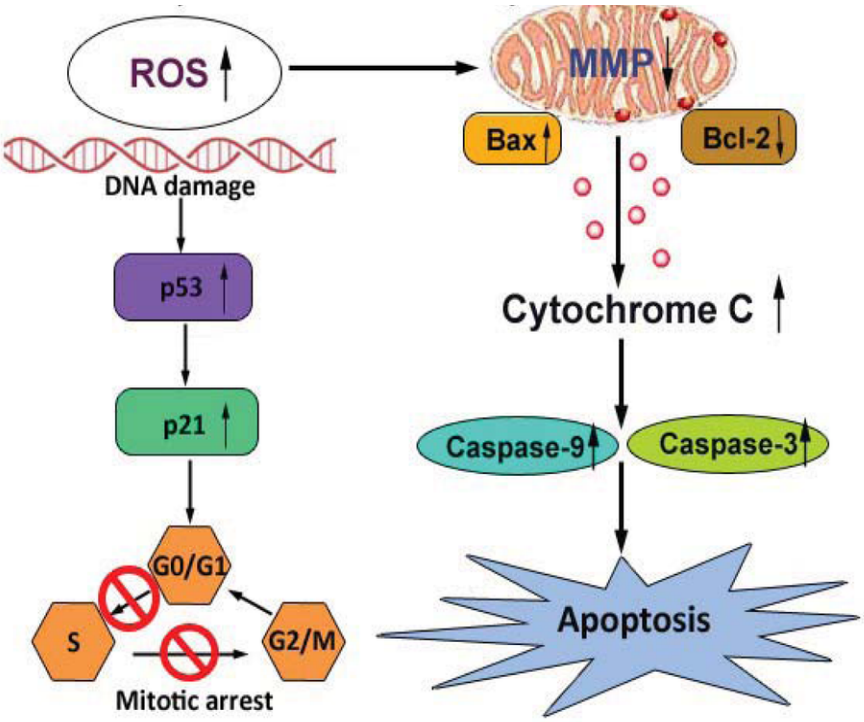

Figure 1.8: Genregulation of *p53*, *Bax* and *Caspase 3* when apoptosis are induced. All three genes are up-regulated. The figure is modified after [71].

1.5 Cells defense mechanisms

Cells have different mechanisms to protect DNA and other macromolecules against oxidative stress. One of these mechanisms is a physical barrier to minimize the availability of oxygen for production of ROS (see 1.2). Another barrier are antioxidants [72].

Antioxidants are defined as chemicals that neutralize and interact with free radicals, thus preventing them from causing damage. Antioxidants are also known as ”free radical scavenger” [72, 73]. The most frequently used antioxidants in the defense against ROS, is amino acids and vitamins [74, 75]. There is a desire to develop new and better modalities including antioxidant therapy. One of the suggested antioxidants that have been discussed is N-acetylcysteine amide (NACA). NACA is a derivate from antioxidant N- acetylcysteine (NAC) [76]. NAC is a popular thiol antioxidant in clinical settings, and has been tested to characterize oxidative stress. It has been described as more effective than vitamin C, vitamin K, and lipoic acid. NAC is used as replenishment of GSH in addition to scavenger ROS [77]. NAC is clinically used as an antidote to paracetamol in case of an overdose situation [77].

NAC is used in treatment of infections, genetic defects and metabolic disorders, including HIV infection [76]. Despite some promising results of NAC, scientists have invented a similar molecule, N-acetylcystein with an amide-group (NACA) (**figure 1.9)**, which is more lipophilic and more permeable through the biological barriers such as the blood-brain-barrier and other biological membranes, like the mitochondrial membranes [78]. NACA is a lipophilic thiol, that gives improved bio-availability and membrane permeability to replenish GSH status of the cell. In NACA, the carboxyl group is neutralized by amino group to improve the lipophilicity and membrane permeability. Studies have shown that NACA could cross the blood-brain barrier as well as biological, especially mitochondrial membrane [76, 79].

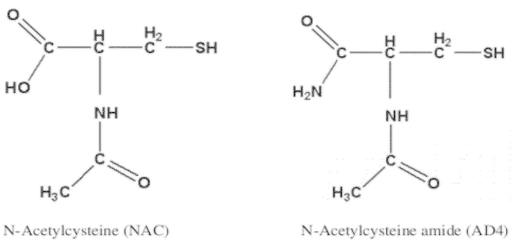

Figure 1.9: Present the structure of N-acetylcysteine (NAC) and N-acetylcysteine amide (NACA [80].

1.6 Cell free DNA (cfDNA) as novel non-invasive biomarker

1.6.1 Characteristic of cfDNA

cfDNA is a product that enters in the circulation when a cell dies, whether by necrosis or apoptosis [81]. Increased level of circulating in blood is considered to be a potential biomarker for cancer [82-84]. Levels of cfDNA are also observed to be increased in other clinical situations for instance trauma, stroke, pregnancy, and premature infants [85-87]. Thus, we suggest that the mechanism generation of cfDNA may be similar to those toward in other stress related diseases, including neonates with asphyxia. Hence, cfDNA could be an interesting potential biomarker.

cfDNA was first discovered in 1948, and was first recognized in 1977 in the blood of cancer patients [88]. cfDNA is defined as extracellular DNA occurring in blood, and has been determined in plasma and serum [89]. The term "free DNA" refers to the compound of DNA fragments detectable in various body fluids. In addition to plasma and serum are cfDNA detected in urine, cerebrospinal fluid, saliva, and feces [81].

cfDNA is mostly a double stranded molecule and the fragment has lower molecule weight than genomic DNA [86]. The fragment length is about 140 to 170 base pairs (bp) and they are present in only few thousands amplifiable copies per milliliter blood [90]. Normal concentrations of free DNA in healthy individuals vary from 0-100 ng/ml, on average 30 ng/ml [83, 86]. The article of Wu.T.L et al [91] reported difference between female and male at different ages. The results indicate that both children and older individuals had slightly higher concentration of cfDNA regardless of sex. However, there was slightly higher concentration of cfDNA in males in comparison to females (**figure 1.10**). In healthy individuals, the main part of cfDNA is found adsorbed to the surface of the blood cells. cfDNA molecules are arranged in nucleosome complex containing DNA fragments and histones [86].

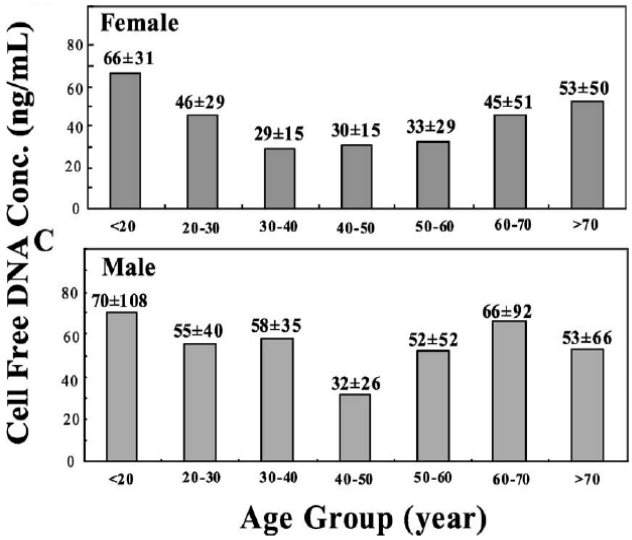

Figure 1.10: Comparison of concentration of cfDNA in male and female. The concentration (ng/ml) is measured for different age groups [91].

In the past, the detection of generally low cfDNA concentration in the plasma of healthy people could not be reliable. These were caused by the low analytical sensitivity of the method used for detection [86, 92]. However, the development of techniques such as PCR and assays with fluorescent dyes resulted in detection of cfDNA concentrations in healthy people [93]. The potential diagnostic and monitoring significances of cfDNA has been demonstrated from different insults [93, 94].

1.6.2 cfDNA in the context of cancer

Apoptosis, necrosis, and circulating tumor cell lysis, produce DNA leakage to bloodstream, resulting in cfDNA in blood (**figure 1.11**) [82, 95]. Total cfDNA has been used as biomarker for early cancer detection [85]. Higher concentration of cfDNA is reported in several types of cancer diagnosis such as breast, lung and prostate cancer has been mostly studied [86].

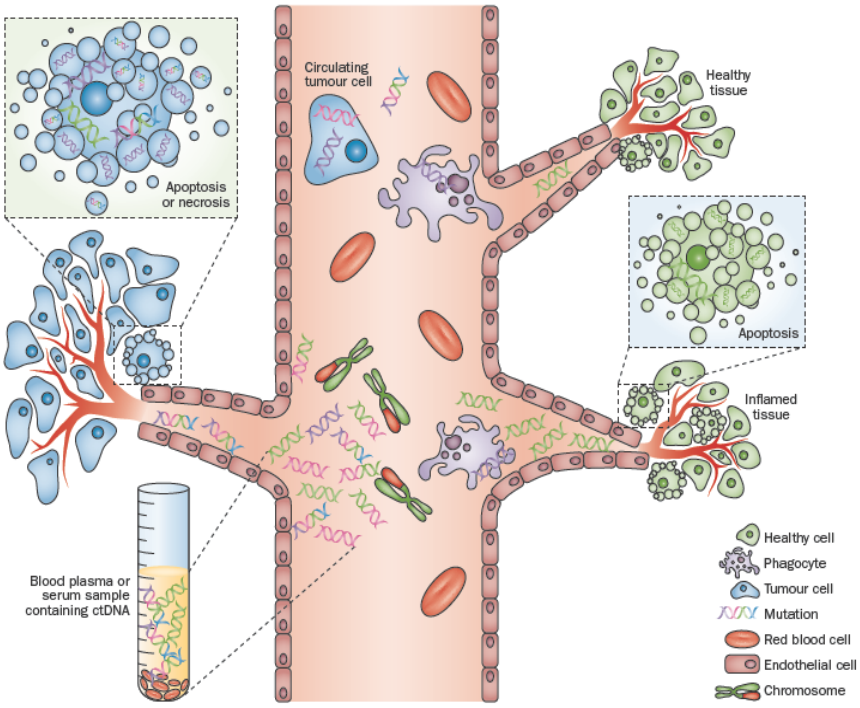

Figure 1.11: Schematic representation showing of circulating tumor cells and circulating cfDNA. cfDNA is presented only in plasma or serum [96] **.**

Increased concentration of cfDNA in plasma from cancer patients revealed the characteristics of tumor DNA. This includes decreased strands stability, the presence of specific oncogenes, tumor suppressor genes, and microsatellite alterations [91]. The size distribution of the plasma DNA obtained from cancer patients varies among samples. The circulating cfDNA in cancer patients might contain tumor DNA as little as 3% to as much as 93% [91]. Measurement of cfDNA has the potential of replacing DNA from invasive and laborious tissue biopsies. Obtaining cfDNA not only requires a non–invasive procedure, but can also be sampled frequently [86, 97].

1.6.3 cfDNA in blood plasma neonates and maternal blood

cfDNA circulates freely in maternal blood stream. Analysis of cfDNA is used for the purpose of non-invasive prenatal diagnosis of fetal sex orfetal Rhesus status (**figure 1.12**) [81]. It has been shown that fetal DNA in maternal plasma is useful to detect certain fetal diseases and pregnancy-associated complications [98].

To our knowledge studies related to cfDNA in the neonatal period has previously been only published once of Tuvea et al [87]. It has been suggested to investigate cfDNA as

biomarker in premature neonatal [87]. cfDNA concentration in the blood plasma of premature neonates is increased significantly compared with term babies (control group).

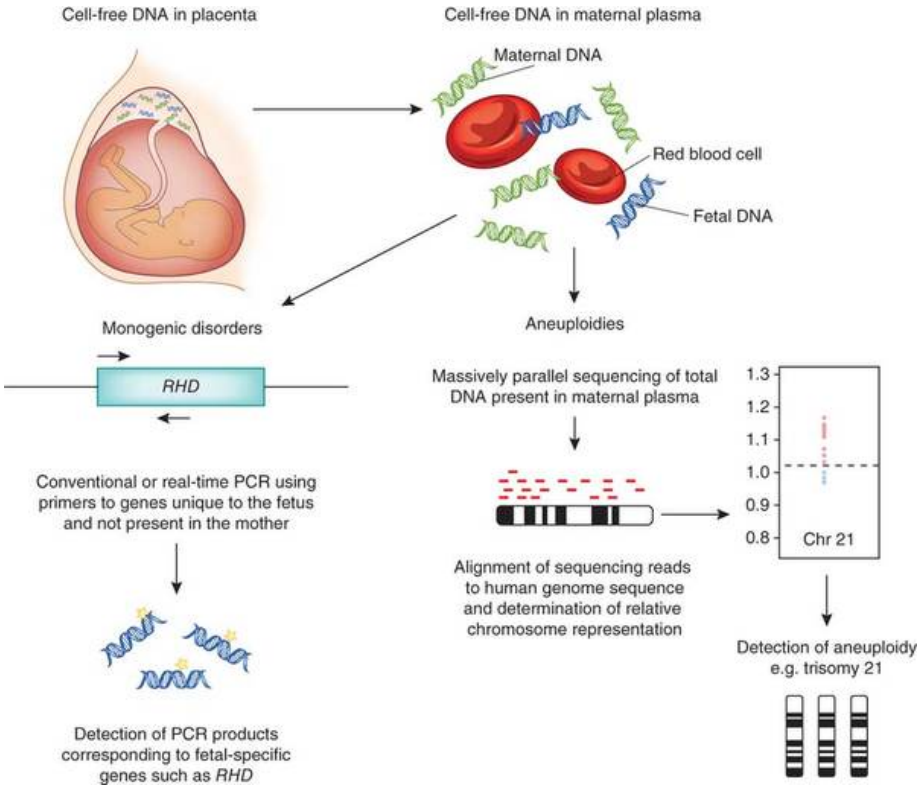

Figure 1.12: Both cfDNA and maternal DNA are represented in plasma. The figure shows a non-invasive method to detect fetal-specific genes such as RHD [99] .

2.0 Aims of the study

The aim of this thesis was to establish novel biomarkers to measure asphyxia damages in a piglet model. Several biomarkers were investigated, including, random mutation capture (RMC), expression of marker genes, and changes in the quantity of cfDNA. In addition a potential protective effect of the antioxidant NACA, against oxidative cell damage, was investigated. In detail:

I. RMC: Develop a rapid and reliable method to investigate mutation in a variety of tissues, cells and experimental settings to measure degree of damage after oxidative stress:
- Establish RMC method to measure DNA damage in mtDNA and ntDNA
- Find an optimal range for stress reaction, hence, concentration and time points to measure DNA damage
- Find an optimal gene and restriction site for mtDNA and ntDNA

II. Investigate the expression changes in various stress related genes

III. Investigate NACA as a protective antioxidant

IV. cfDNA: Establish novel techniques applicable to small amounts for a fast, less-invasive and independent analysis of oxidative damages in newborns piglets and humans.
- Measure concentration of cfDNA in piglets exposed to hypoxia
- Find a reliable method to extract and measure cfDNA
- Find a standard to use for measurement of cfDNA
- Investigate the difference between cfDNA measurement photometric and qRT-PCR
- Investigate the difference between adult and newborn pigs and pig versus human

3.0 Materials

3.1 Cell culture

Porcine epithelial-like embryonic EFN-R kidney cell line was collected at the Friedrich-Loeffler Institut, Federal Rescarch, Institute for Animal Health, Greifswald-Insel Riems, Germany. EFN-R cells were grown using Dulbecco´s modified eagle´s medium (DMEM) (sigma-lifescience, USA), 10% fetal bovine serum (FBS) and 1% streptomycin (sigma-lifescience, USA). The cells were incubated in a cell chamber at 36.8°C and 5% CO_2. Cells were cultured when they were approximately 80% confluent. The confluence describes the percentage of cells in growth.

Subculturing: Cells were washed with PBS, trypsinated and incubated in the cell chamber for 3 minutes. Cells were then centrifuged at 3000 rpm for 3 minutes, and the pellet was dissolved in fresh cell medium.

A Bürker chamber was used to calculate cell numbers. 100 µl of cell suspension together with 900 µl trypan blue solutions (life- technology, UK) was added onto a Bürker chamber glass plate and covered with a slide and placed under a microscope. The amount of cells was counted in minimum of five squares, and the average value of number of cells per square was calculated. The cells were counted only on the top and the left edge of each square, to avoid cells be counted twice. The desired amount of cells was adjusted and transferred to plates for further experiments.

3.2 Animal studies

In the present work, a total 80 newborn piglets (12-36 hours) have been used for hypoxia and reoxygenation testing different antioxidative protective agents. Piglets belonged to a race of pigs called Noroc, a crossbreed between Norwegian landrace (50%), Norwegian yorkshirepruke (25%) and duroc (25%) [3]. Blood, urine, and cerebral spinal fluid (CSF) were collected together with tissue samples from organs like brain, liver, and kidneys. The piglets were exposed to different combination of treatments with hypoxia (8% O_2) followed by reoxygenation (21% O_2), and various potentially neuroprotective agents treatment, like NACA and hypothermia.

Cohort 1: The experiment was divided in five different groups:

Group 1 - Severe hypoxia:

The pigs were exposed to 8% O_2 until Base Excess (BE) reached -20 mmol/l or blood pressure was below 20 mm Hg. Immediately after hypoxia the piglets received saline.

Group 2 - Severe hypoxia + NACA:

Severe hypoxia performed like in group 1. Piglets immediately received NACA instead of saline.

Group 3 - Moderate hypoxia:

The pigs were exposed to hypoxia at 8% O_2, but only until a BE of -15 mmol/l was reached. The piglets received saline.

Group 4 - Moderate hypoxia + NACA:

Moderate hypoxia was performed like for group 3, and piglets immediately received NACA instead of saline.

Group 5 – Control group

This group of piglets was not exposed for hypoxia.

Plasma samples were collected in five different time points: Start Hypoxia, End Hypoxia (0 minutes), 30 minutes, 270 minutes and 570 minutes after reoxygenation. CSF was collected at the end of the study.

Cohort 2: Experiment was divided in three different groups.

Group 1 - Severe hypoxia: Hypoxia:

The pigs were exposed to 8% O_2 until Base Excess (BE) reached -20 mmol/l or Blood pressure fell below 20 mm Hg. The piglets received saline after hypoxia.

Group 2 - Severe hypoxia + Hypothermia:

Severe hypoxia was performed as group 1. The hypothermia treatment started 30 minutes after start hypoxia.

Group 3 - Control:

This group of piglets was not exposed for hypoxia.

Plasma samples were collected after start hypoxia, end hypoxia (0 minutes), 30 minutes, 210 minutes and 540 minutes after reoxygenation (21%).

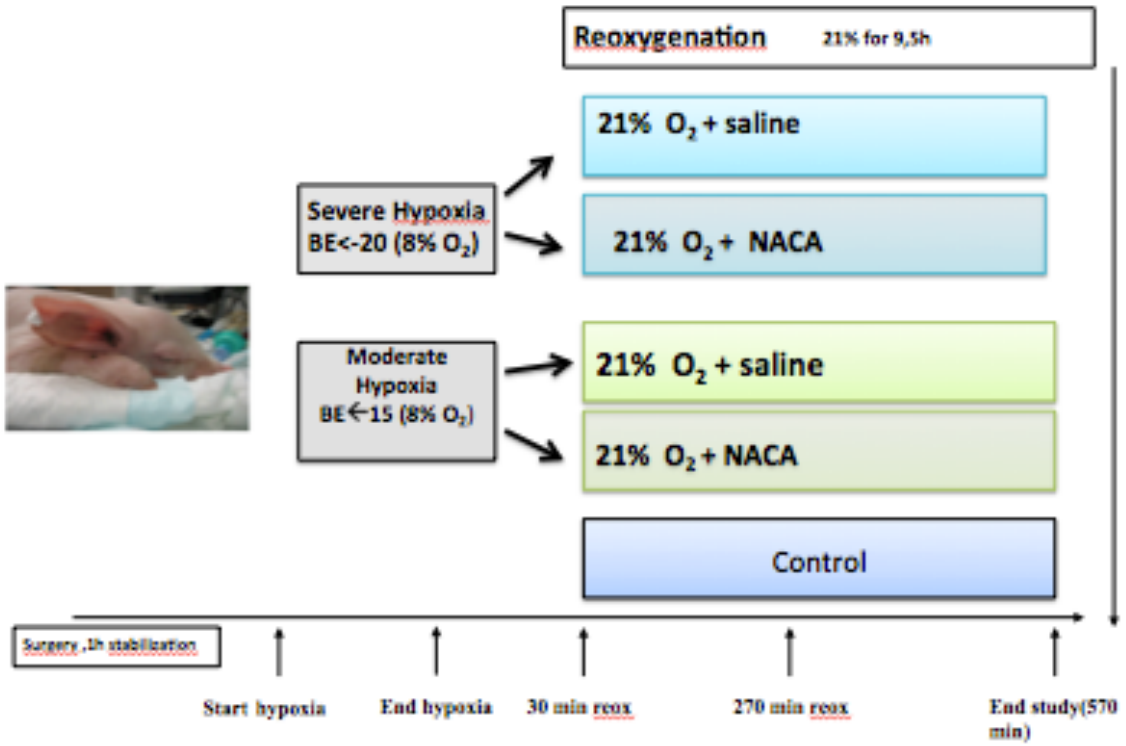

Figure 3.1: Cohort 1. Schematic representation of the experiment with NACA treatment.

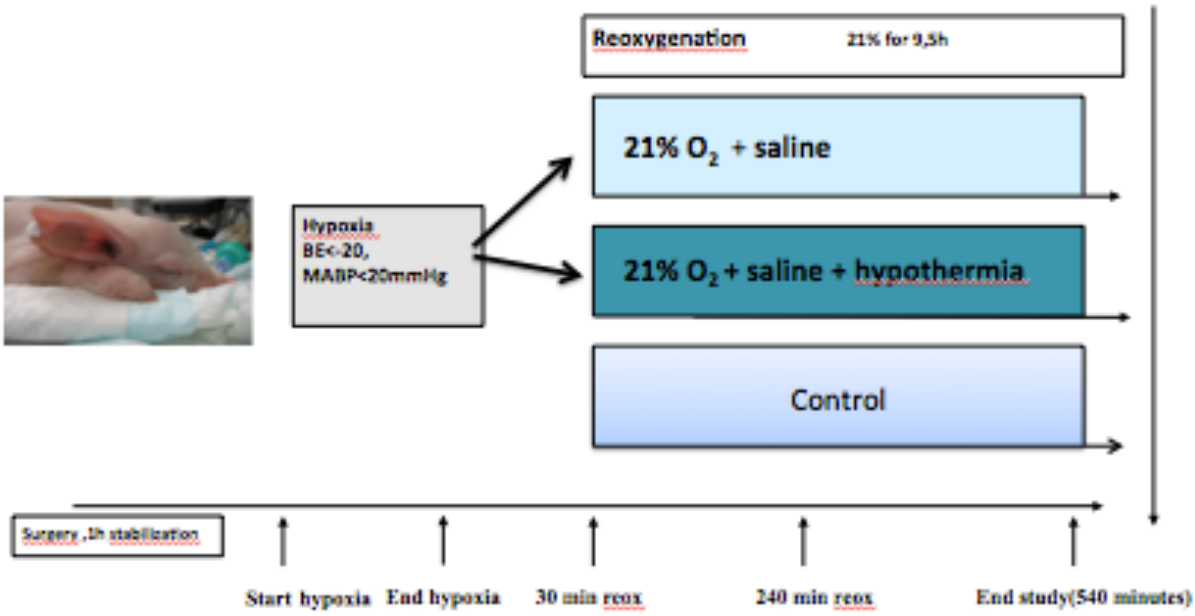

Figure 3.2: Cohort 2. Schematic representation of the experiment with hypothermia.

3.3 Kits

Name	Area of use	Supplier	Country
Wizard® Genomic DNA	DNA isolation	Promega	Madison USA
DNeasy® Blood & Tissue Kit	DNA isolation	Qiagen	California, USA
NucleoSpin ® Plasma XS	DNA isolatin	Macherey-Nagel	Düren, Germany
KingFisher Pure Kits	DNA isolation	Thermo scientific	Vantaa, Finland
E.Z.N.A Total RNA Kit II	RNA isolation	Omega bio-tek, VWR	USA
RNase- Free DNase I set, 50 preps	cDNA	Omega bio-tek	Norcross, Georgia
BioRad DC protein Assay	Protein concentration assay	Bio- Rad Laboratories	CA, USA
ECL prime western blotting	Detection reagent	GE Healthcare	Italy

3.4 Antibodies

Name	Source	Concentration	Supplier
Primary antibody			
Anti BAX (N-20)	Rabbit	200 µg/ml	Santa cruz Biotechonology
β-actin (I-19)	Goat	2 µg/ml	Santa cruz Biotechonology
Seconday antibody			
Anti Rabbit- IgG-HRP	Goat	1:2000	Southern biotech
Anti Goat (SC-2020)	Donkey	1:5000	Santa cruz Biotechonology

3.5 DNA standards and enzymes

Name	Stock concentration	Suppler
1 kb DNA ladder	100 µg/ml	AB gene
BfoI enzyme	200 µl	Thermo scientific
Cut Smart buffer	10X	Thermo scientific
Fast digest buffer		New England, biolabs
HaeII eznyme	20.000 U/ml	New England, biolabs
Human genomic male DNA	172 µg/ml	Promega
Porcine DNA (Control genomic DNA)	0.53 µg/ul	Ambsio
Salmon sperm	50 mM	Sigma life science
TaqI enzyme	1000 U	Thermo scientific

3.6 Chemicals

Name	Chemical formula	Supplier	Country
0.05% Trypsin – EDTA		Sigma, life science	USA
abosolutt alkohol prima		Sigma, life science	USA
Acetic acid	CH_3COOH	Merck	USA
Bovine serum Albumine (BSA)		Bio-Rad	USA
Dimethyl sulphoxide (DMSO)		Sigma, life science	USA
DMEM		Sigma, life science	USA

DNase		Omega	USA
Dry milk powder		Bio-Rad	USA
Electran Agarose		VWR, prolabo	USA
Ethanol (EtOH)	C_2H_6O	Antibac	Norway
PBS- bio whittaker		Lonza, verviers	Belgium
Gel load 6x		AB gene	UK
GelredTM Nucleic Acid		Invitrogen	UK
Glucose	$C_6H_{12}O_6$	Sigma-Aldrich	USA
Hydrochloric acid	HCl	Sigma life-science	USA
Hydrogen peroxide 30%	H_2O_2	Sigma life-science	Germany
MTT		Sigma life-science	USA
N-Acetyl-L-cysteine amide (NACA)		PharmaZell gmBH	Germany
PBS		Biowhittaker	Belgium
Power SYBR Green PCR Master Mix		Applied Biosystems	USA
Proteinase K		Qiagen	USA
RNAase		Bio-Rad	USA
SYBR® Gold Nucleic Acid Gel Stain		Invitrogen	UK
Trizma base	$C_4H_{11}NO_3$	Sigma, life science	USA
Tween 20		Sigma, life science	USA
β-Mercaptoethanol	$C_2H_8O_5$	Applichem	Germany

3.7 Technical equipment

Equipment	Model	Manufacturer
Burker chamber	0.100mm	Assitent
Cell chamber	Galaxy 170R	New Brunswick
Cell flask	NUNC (nunclon treated flask, blue filter cap)	Roskilde
Centrifuge	Sorwall RT6000B	
Centrifuge	Megafuge 1.0	Heraeus instrument
Centrifuge	Biofuge fresco	Heraeus instrument
Cover glass	20X20mm	VWR
Dispoable serological pipets		Fisher scientific
ED heating immersion circualtor		JULABO GmbH
Electrophoresis	Powe Pac 300	Bio-rad
Extractor	KingFisher Duo	Thermo scientific
Filter paper		
Gel imaging	G:box, Syngene	VWR
Microplates	96 well ELISA microplates	Greiner bio-one
Microscope	Lecia DM IRB	
Microtubes	Axygen	
Multimode plate reader	Victor^{TM} X3	Perkin Elmer
Multiskan Acent	V2.6	Thermo Electron corporation
Nunc plate		Thermo scientific
Optically clear Adhesive seal sheets	AB-1170	Thermo scientific
PCR Tubes	PCR-02-C	Thermo scientific

Pipette tips	Biotix	
pipettes		VWR
qRT- PCR	Applied biosystems Viia7	Life technologies
Realtime- PCR	7300 real time PCR system	VWR
Spectrophotometer	NanoDrop (ND-100)	Life Science
Sterile tube	Sarstedet	
Thermo fast 96 detection plate	AB-1100	Thermo scientific
Thermo shaker	PHMP	Grant- bio
Thermo-shaker	TS- 100	bioSan
Thermocycler	PTC-100™ programmable Thermal Controller	MJ Research, INc
Vortex	MS1 Minishaker	Sigma-Aldrich

4.0 Methods

4.1 Cell lines

4.1.1 Cell line experiments

Cells were used as model system for stress experiments. 150 000 cells were seeded in each well in a 12-wells plate. The cells were starved for 24 hours and the confluent cells were treated with hydrogen peroxide (H_2O_2) for various incubation time and concentrations.

Experiment I:

In experiment I (**table 4.1**) the cell plate was divided into 4 groups with triplicate, each group was treated with different concentration of H_2O_2 (Sigma life science, Germany).

Table 4.1: Experiment I were divided in four different groups.

Group 1 (control group)	Without H_2O_2
Group 2	50 µM H_2O_2
Group 3	100 µM H_2O_2
Group 4	200 µM H_2O_2

Experiment II:

In experiment II were cells treated with H_2O_2 and NACA (PharmaZell GmbH, Germany). The experiment was divided into five groups, as described in table 4.2.

Table 4.2: Experiment II, cells treated with NACA.

Group 1 (control group)	Without H_2O_2 or NACA
Group 2 (control H_2O_2)	100 µM H_2O_2
Group 3 (control NACA)	750 µM NACA
Group 4 (pre-treatment)	Cells were first treated 1 hour with 750 µM NACA, followed by 100 µM H_2O_2
Group 5 (post-treatment)	Cells were treated with 100 µM H_2O_2 in 1 hour before 750 µM NACA was added

4.1.2 MTT viability assay

The cell viability for experiments described in 4.1.1 was measured by the MTT assay (Sigma Aldrich, USA). The MTT (3,4,5 dimethylthiazol-2,5 diphenyl tetrazolium) viability assay is based on the ability of mitochondrial dehydrogenase enzymes in living cells to convert MTT to a purple formazan precipitate [100]. These mitochondrial succinate dehydrogenases may reflect the number of viable cells present. The resulting crystals are subsequently dissolved using dimethyl sulfoxide (DMSO) and the optical density of each well is measured using a mulitscan acent plate reader (Thermo Electron corporation, USA). Cells were exposed to H_2O_2 for 1 hour and 24 hours. After incubation, the medium was removed and 200 µl MTT was added and incubated for 1 hour. MTT was removed and 100 µl of DMSO was added. The plate was analyzed in a mulitscan acent plate reader at optical density of 550 and 595 nm.

4.2 DNA extraction methods

4.2.1 Isolation of DNA in cells

Cells were treated with H_2O_2 for 15, 30, or 45 minutes. Prior to treatment, cell medium with serum was replaced with new fresh serum free medium, to avoid inactivation of H_2O_2 by serum.

Adherent cells were harvested by adding lysis-buffer and phosphate-buffered saline (PBS). Briefly, cells were first washed with PBS, and lysated with 100 µl DNA lysis buffer and 200 µl PBS. Cells were harvested by using a cellscraper. Replicates were transferred to a new eppendorf tube.

DNA was isolated with KingFisher Blood DNA kit using KingFisher Duo extractor (Thermo scientific, Finland). KingFisher Duo is an isolation extractor based on magnetic beads. The initial step in isolation of DNA is lyses of the cells. The next step (wash steps) includes dispose of proteins, cell debris, and any residual contaminants, while the DNA is bounded to magnetic beads. Finally the DNA was eluted in a total volume of 80 µl.

4.2.2 Isolation of DNA in cerebellum

Total DNA of cerebellum was isolated using DNA blood and Tissue kit (Qiagen, USA) according to manufactures protocol with modifications. In brief, 10-25 mg of cerebellum tissue was lysed and dissolved. The process of lysis is based on addition of 180 µl buffer ATL and 20 µl proteinase K, as well as incubation at 56°C over night. Further, the procedure is identical to the description in section 4.2.3. Concentration and purity of DNA was assessed by NanoDrop ND 100 (Life Science, USA) and diluted to a final concentration of 6 ng/µl and 15 ng/µl DNA.

4.2.3 Extraction of cfDNA

Several methods exist to extract cfDNA from blood samples [95]. Existing methods were compared in order to find the kit with best reliable result.

Following kits were tested:

1. Qiagen blood and Tissue kit (California, USA)
2. Macherey-Nagel, Nuleospin Blood kit (Duren, Germany)
3. Promega, Wizard® Genomic DNA (Madison, USA)

cfDNA was measured in plasma and CSF from pig samples. Blood samples were centrifuged at 2500 rpm for 10 minutes with a temperature set at 4°C. The supernatant, containing the plasma with cfDNA was transferred to an eppendorf tube.

The kits from Qiagen and Macherey-Nagel are based on silica-based spin columns with the ability to bind DNA. For the Qiagen kit, 240 µl plasma sample was used as start volume, followed by proteinase K treatment and buffer AL. The samples were incubated at 56°C for 10 minutes. 200 µl 100% ethanol was added, and the mixture was transferred into a DNeasy Mini spin column placed in a 2 ml collection tube and centrifuged at 8000 rpm for 1 minute. The spin column was placed in to a new 2 ml collection tube and processed in two separate wash steps with buffers AW1 and AW2. Finally the DNA was eluted by adding 200 µl buffer AE to the center of the spin column membrane and centrifuged for 1 minute at 8000 rpm.

The Nucleospin® plasma XS kit from Macherey-Nagel, is based on a similar mechanism like the Qiagen kit. The start volume was 240 µl and proteinase K was added before incubation at 37°C for 10 minutes. The binding condition was adjusted with binding buffer (BB). Sample was centrifuged at 11 000 g, to induce DNA-binding to the silica membrane. The silicon membrane was washed with washing buffer (WB) and DNA eluted with 20 µl elution buffer. Finally the samples were incubated at 90°C for removale of residual ethanol.

Wizard® genomic DNA purification kit is based on a four-step process. First step is purification procedure where nucleic acid is lysed, followed by RNase digestion. The proteins were removed by a salt-precipitation step. The final step is desaltation of DNA by isopropanol precipitation. 220 µl was used as an initial volume for Wizard® kit. Identical volume of nuclei lysis solution was added.

cfDNA concentrations and DNA purification were measured by using NanoDrop-ND 100. The ratio of absorbance at 260 nm and 280 nm gives an indication of the purity of DNA. A ratio of 1.8 is generally accepted as pure DNA. The DNA concentration is estimated in a wide range from 0.4 to 15 000 ng/µl. The NanoDrop spectrometer is therefore only used on high concentration samples.

4.3 DNA quantification

4.3.1 DNA standard

Several different DNA sources were tested to prepare a standard curve for measuring cfDNA concentration. In the literature standard curve is prepared with commercial salmon sperm DNA [101]. The commercial salmon sperm (Sigma life science, Japan) was diluted with PBS to various concentrations (5000, 2500, 1250, 1000, 750, 250, 150, 125, 100 ng/ml*)*. In addition to salmon sperm DNA, a DNA standard with Human genomic DNA male (Promega, USA) was also prepared, using the same dilution steps.

In our study however, most samples were from pigs. A new standard was therefore prepared with DNA from porcine. The DNA was diluted with PBS to following concentrations: 1250, 750, 500, 250, 125, 100, 75, 50, 25, 12.5, 6.25, ng/ml.

Fragmentation

cfDNA in plasma consist of short fragments (ca. 200 bp) [92]. However, the porcine DNA used as standard had a higher fragment size and was fragmented prior to cfDNA measurement. This was done in two different ways:

I. Fragmentation of DNA into small fragments by incubation of porcine stock in UV-bath for 5 minutes and then followed by a serial dilution.
II. Fragmentation of DNA with restriction enzyme, HhaI. The reaction mix contained 3.5 µl of 0.53 µg/µl porcine DNA and 1 µl smart cut buffer, 5 U HhaI enzyme and MQ water to a final volume 10 µl. The DNA was digested for 1 hour at 37°C and inactivated in 10 minutes at 65°C. After fragmentation the stock was diluted with PBS to various concentrations.

Recovery test

A recovery test was done to investigate DNA recovery after extraction. The purpose was to test recovery of the Qiagen kit. Plasma from pigs was used, and extracted together with 100 ng/µl standard. Both 100 ng/µl standard from porcine and human was used in two separate plasma samples. Plasma samples were also treated with Dnase (Bio-Rad, USA) and extracted with Qiagen kit. The samples were measured fluorometric (VictorTM X3, Perkin Elmer) using SYBR® Gold (Invitrogen, Paisley, UK).

4.3.2 Photometric method

cfDNA was detected with fluorochrome SYBR® Gold directly in extracted plasma samples and CSF. SYBR® Gold is similar to other SYBR dyes, for instance SYBR green I stain and SYBR green II stain. DNA binding dyes bind reversibly to DNA by intercalation, minor groove binding, or a combination of both. The unsymmetrical cyanine has two fluorescence excitation maximas when it binds to DNA; one at 300 nm and one at 495 nm. SYBR® Gold stain is more sensitive than SYBR green I and II -stain

when it comes to detecting double stranded DNA, single stranded DNA, and RNA [102].

SYBR® Gold Nucleic Acid Gel Stain was diluted first at 1:1000 in dimethyl sulphoxide (DMSO, Sigma-Aldrich, USA) and then diluted 1:8 in PBS. 10 µl of DNA was applied to a black 96 well plate and 40 µl of diluted SYBR® Gold was added. Fluoroscens was measured with a fluorometer (VictorTM X3, Perkin Elmer) at an emission wavelength of 535 nm and excitation wavelength of 485 nm [101]. Concentration of unknown samples was calculated from the standard curve by extrapolation in a linear regression model. Usually, the goodness of fit of the standard curve (R^2) was higher than 0.97.

4.3.3 qRT-PCR

Designing optimal primers is essential to obtain successful PCR reaction. The following criteria should be accomplished [103].

I. The length of the primers should be between 18 bp and 30 bp.
II. The primer should not form hairpin loops.
III. The primer should not become complementary with itself (homodimers).
IV. The primer should not become complementary with the opposite primer (heterodimer).
V. An equal amount of purines and pyrimidine's is an advantage.
VI. The GC content of the primer should exceed 40% to ensure good binding of primer to the template.
VII. The primer should not have pseudogenes, mutation or repetitive elements (tandem repeats).

In a PCR reaction, the efficiency of the reaction should ideally be 100%, meaning that the template doubles after each cycle during exponential amplification. The criteria's mentioned above could all influence the efficiency. To evaluate the efficiency a 10-fold dilution of template was run for each set of primers. A good reaction should have an efficiency of 90-100%, which corresponds to a slope of between -3.58 and -3.10. An optimization test with various primer- and template- concentrations (0.5 uM, 1.0 uM, 1.5 uM and 2.0 uM) were also made.

Table 4.3: Table below shows a list of primers used in this study for DNA in qRT-PCR. The primers were designed based on the criteria's mentioned above and with the respect to primer design tool: primer 3 plus, Viia 7 and BLAST.

Gene	Forward primer (5'-3')	Reverse primer (5'-3')
HMBS_L	GCTTCAGAGAAAGTTCCCACA	GGCCTTCTGGACCTCATTT
PMM1	GAGATTCCCTGGAGCTGTGT	ATTCTGTCCGCTTTGTTCCT
Beta-globulin	GCAAGCTGCTGGTTGTCTAC	GTCACTGAAGGACTGGAGCA
HMBS_S	GTAGACCATGGATGGCAGTG	GTCACTGAAGGACTGGAGCA
mt DNA 12S_target	CGCAACTGCCTAAAACTCAA	TAGCCCATTTCTTTCCAACC
mt DNA 12S_Control	AGGAGCAGGTATCAAGCACA	ACTCTTTACGCCGTGGATCT
p53	CGCCATGGCCATCTACAAG	GCCCACTCACCATCGCTATAG

Quantitative real time PCR (qRT-PCR) is based on the polymerase chain reaction where a DNA sequence is amplified exponentially during repeated cycles of heating and cooling. The key to qRT-PCR is the modification, which enables us to monitor the progress of the amplification as it is taking place [104]. Template is detected by the binding of a fluorescens-dye that interacts with dsDNA. The amount of product (cycle threshold) can be measured by the fluorescent-light emitted from the fluorescent-dye interacting with synthesized dsDNA. The cycle threshold (ct) value is the number of cycles that is required for the fluorescent signal to overcome the threshold.

cfDNA from both plasma and CSF, including porcine DNA standard, were analyzed by qRT-PCR. The samples were run with the genes previously described in table 4.3. The mixture containing 5 µl DNA samples of plasma or CFS, and standards (6.25-1250 ng/ml) and 2 µl of each primer (20 µmol/l), 12 µl SYBR mix and MQ-water to a final volume of 25 µl. The reaction was carried out in Applied biosystems Viia7 qRT-PCR (Life technologies, USA).

Table 4.4: Standard qRT-PCR program used in these thesis.

	Temperature	Time	
Initial activation step	95°C	10 min	
Denaturation	95°C	15 s	X 40
Annealing	60°C	60 s	
Extension	95°C	15 s	

4.4 DNA damage

4.4.1 The RMC method

RMC method was established and described previously in Vermulst et al [105]. RMC is a method where specific primer and restriction enzyme are used to determine the mutation rate. The method is based on the ability of damages/mutations to inhibit restriction enzyme cleavage. The assay revolves around restrictions enzyme used in the different genes, TaqI or BfoI, which is used to discriminate between wild type (WT) DNA and rare DNA molecules that contain a mutation in the restriction site. By digesting the mtDNA and ntDNA with enzyme, the DNA molecules will be cleaved at a known restriction site (**figure 4.1**). However, a small number of molecules will be resistant to the restriction cleavage due to a mutation in the restriction site. The whole molecule can be quantified with qRT-PCR using primers that flank the restriction site [105].

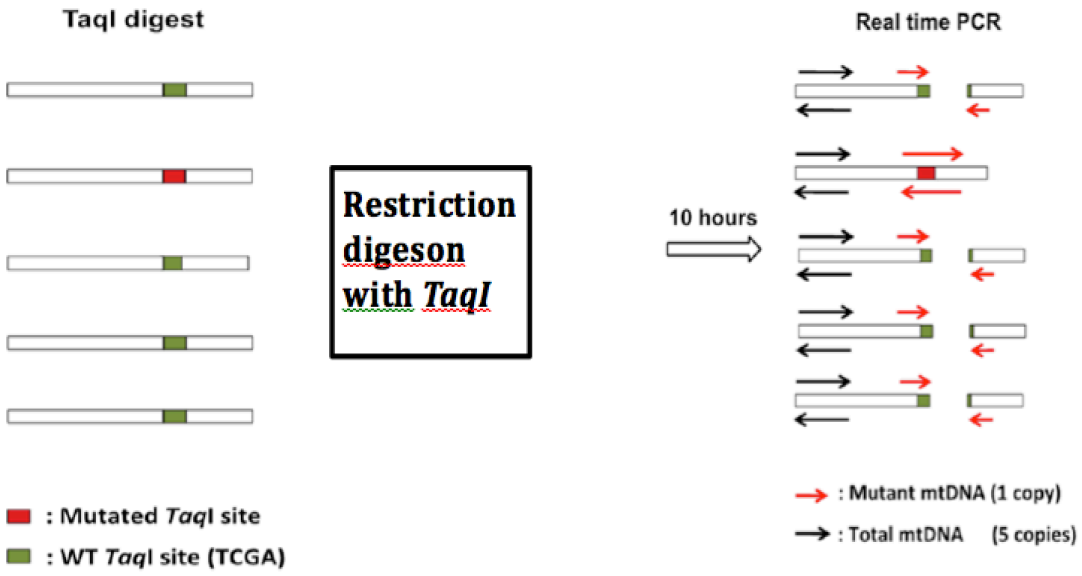

Figure 4.1: Restriction digest with TaqI enzyme in mitochondrial *12S* gene. TaqI digest in mtDNA in mutant and WT. The digest was performed in qRT-PCR as described in section 4.1.

In qRT-PCR the WT and the mutant will come at different ct-value. The mutant that is the "uncutted" product will have a higher ct-value than the WT that is "cutted" (**figure 4.2**).

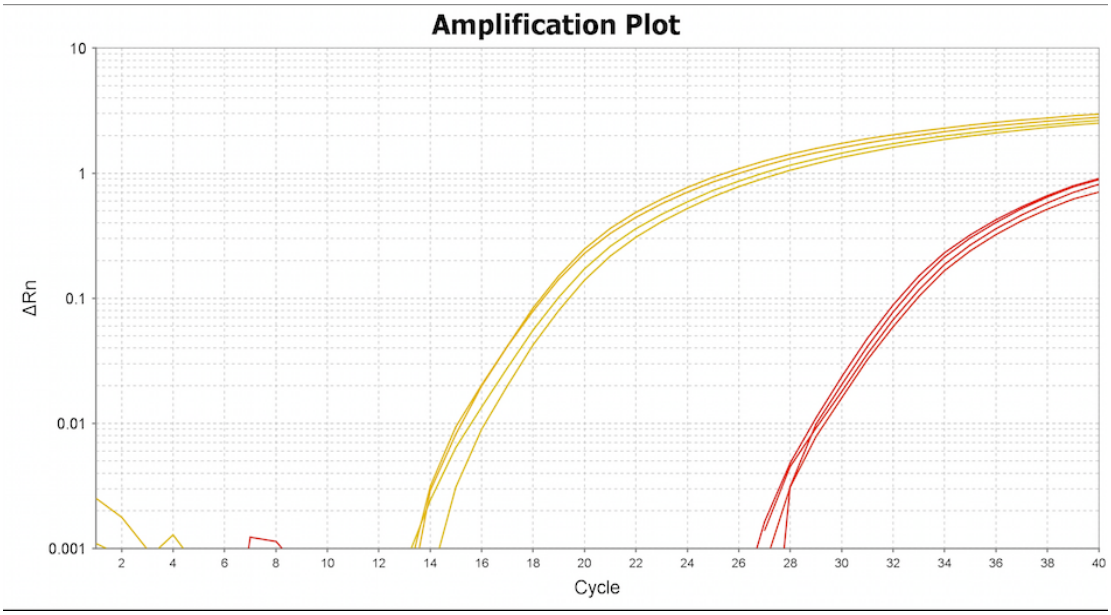

Figure 4.2: Amplification plot of the *12S* target and *12S* control gene at qRT-PCR. The red curve indicates mutated or damaged DNA, and is the "uncutted" product. The mutated/damaged product of DNA will have a higher ct-value than WT. The damaged will be calculated with ΔΔct method.

4.4.2 Enzyme test

A number of tests were performed to control whether the restriction enzymes worked properly. To confirm that the primers were correct, the primer efficiency was calculated by setting up a 10-fold curve at qRT-PCR with test samples.

Plasmid (pet101) and PCR product from EFN-R cells and cerebellum was tested to control if the product showed correct fragment size. The test samples for mtDNA were first digested with 1U restriction enzyme TaqI (Invitrogen, Paisley, UK) with smart cut buffer and nuclease free water to a total volume of 30 μl. The restriction digest was performed at 65°C for 15 minutes followed by inactivation of the enzyme for 10 minutes at 95°C. Restriction enzyme BfoI (Thermo Scientific, USA) and fast digest buffer were used for nuclear DNA. The reaction was digested for 5 minutes at 37°C and enzyme inactivation was performed for 10 minutes at 65°C. The digestion product was tested using agarose gel electrophoresis to detect the fragment length for the enzyme treated and non-treated product.

DNA samples were analyzed using a 1% (W/V) agarose gel, buffered with 1 x TAE-buffer. The agarose/buffer mixture was heated and cooled and gel red (biottium, Invitrogen, UK) was added to visualize DNA molecules. The samples were mixed with loading buffer, which increases the density. The gel was visualized with Gel imaging, syngene (VWR, USA).

4.4.3 Analysis of damages at DNA level

The level of DNA damage was analyzed by a qRT-PCR method based on the ability of DNA lesions to inhibit restriction enzyme cleavage. The method is based on the RMC method developed by Vermulst et al [105] with some modifications. Mastermix for one reaction contained 6x SYBR green, 0.5 μM forward- and reverse primer and nuclease free water to a final volume of 20 μl. To mastermix with target *12S* gene (**table 4.3**) 1U TaqI enzyme was added. Instead of PCR amplifying and sequencing every DNA molecule present in a sample, the RMC-assay inserts a simple DNA digestion step prior to PCR amplification, in order to remove WT molecules from further analysis The

digestion step was performed at 15 minutes at 65°C for enzyme digest and 10 minutes at 95°C for inactivation.

ntDNA damage was measured using 20 ng DNA. Unlike analysis of DNA damage in mtDNA described above, the ntDNA was first treated with restriction enzyme. This was because the fast digest buffer inhibited the enzyme in qRT-PCR. Briefly, enzyme-buffer mix was prepared mixing 1U restriction enzyme with 0.5 µl of fast digest buffer. Reaction mix was prepared by mixing 15 ng/µl gDNA with 1 µl enzyme-buffer mix. Volume was made up to 20 µl with autoclaved MQ water. The digestion was performed for 15 minutes at 37°C and 10 minutes at 80°C for inactivation. After enzyme digest, the product was analyzed with qRT-PCR.

DNA damage frequency was calculated using ΔCT method following, 2exp- (ct^{targ} – ct^{ctrl}), where ct^{Targ} and ct^{ctrl} represent CT values of enzyme-treated and non-treated DNA.

4.5 Gene expression

4.5.1 RNA isolation

RNA was isolated from EFN-R cells with E.Z.N.A ® RNA Isolation kit (Omega Bio-Tek, USA), according to manufacture protocols. Briefly, β-mercapthoethanol (Applichem, Germany) was added to total RNA kit (TRK) lysis buffer. 350 µl lysis buffer was added to each well in 12 well-plate and the cells were collected by using a cell scraper. 70% ethanol was added to the sample and applied to a HiBind ®RNA spin column to bind RNA. The sample was centrifuged and washed with wash buffer I. After the first wash step, a Dnase step was performed, where Dnase I digestion mix was added and incubated for 15 minutes at room temperature. The Dnase I digestion mix was prepared with E.Z.N.A Dnase I digestion Buffer (73.5 µl) and Rnase-free Dnase I (20 unit/µl) in a total volume 75 µl. Following DNase treatment, the samples were washed with wash buffer II and centrifuged. This washing and centrifugation steps were performed twice. Finally the RNA was eluted with 40 µl DEPC-treated H_2O. Concentration of RNA was measured with NanoDrop and diluted to 50 ng/µl.

4.5.2 cDNA synthesis

Complementary DNA (cDNA) is double-stranded DNA synthesized from a messenger RNA (mRNA) template in a reaction catalyzed by the enzyme reverse transcriptase. cDNA was prepared from 0.5 μg total RNA using High Capacity cDNA reverse transcription kit (Applied Biosystems, USA). cDNA synthesis was preformed with 0.5 μg of cDNA in a total volume of 40 μl, containing 1x HotStart PCR buffer, 0.2 mM of dNTPs.

4.5.3 Analysis of mRNA expression levels

Gen expression analysis was performed by qRT-PCR using the primer listed in table 4.5. qRT-PCR was performed in a total volume of 16 μl containing 10 μl of Power SYBR green PCR Master Mix (Applied Biosystems, USA), 100 μM primer, 4 μl of cDNA and MQ water. The qRT-PCRs were performed in a 96-well plate. The reactions were carried out in an Applied biosystems Viia7 (Life technologies, USA). The cycle condition is described in table 4.4.

Table 4.5 Table below shows a list of primers used for gene expression. The primers were designed based on the criteria's mentioned above and with the respect to primer design tool: primer 3 plus, Viia 7 and BLAST.

Gene	**Forward primer (5'-3')**	**Reverse primer (5'-3')**
CASP-3	GACGCACAGTGGGACTGAAGA	GCCAGGAATAGTAACCAGGTCG
Bax	AGCGAGTGTCTCAAGCGCAT	ACACCTCTGCAGCTCCATGTTAC
p53	CTCACCATCATCACACTGGAA	TGGGCAGTGCTCGCTTAG
rplP0	ACAATGTGGGCTCCAAGCA	CATCAGCACCACGGCTTTC

The expression was normalized using P_O as an internal control. Each sample was repeated with four independent biological replicates. Gen expression was determined with the ΔCt method and reported as $2^{-\Delta\Delta Ct}$, where Ct represents the threshold cycle.

4.6 Protein expression

4.6.1 Protein isolation

Proteins were isolated from cells treated with 100 µM H_2O_2 and control (without H_2O_2) for 45 minutes, 1.5 hour, 3 hours, or 18 hours. Briefly, the cells were washed with cold PBS before treatment with 200 µl trypsin. After incubation 1 ml cell medium including 10% FBS were added to the wells. Four replicates were transferred to a 15 ml tube and centrifuged at 3000 rpm for 5 minutes at 4°C. The supernatant was removed and the pellet was dissolved in 1 ml PBS and transferred into a new eppendorf tubes. The samples was centrifuged at 3600 rpm for 5 minutes at 4°C. The supernatant was discarded and the pellet was dissolved in 50 µl lysis buffer. The samples were incubated on ice for 30 minutes and centrifuged for 10 minutes at 1300 rpm at 4°C. The supernatant was transferred into to new eppendorf tubes and the protein concentration was measured.

4.6.2 Protein measuring with Bio-Rad DC protein Assay

The protein concentrations of the extracts were estimated with the Bio-Rad DC protein assay (Bio-Rad Laboratories, USA) using bovine serum albumin (BSA) as a standard. Protein standard (BSA, 1.47 mg/ml) was diluted in lysis buffer to a linear range from 0.2 mg/ml-1.5 mg/ml. The samples were measured using a Multiskan acent reader.

4.6.3 Western blot

Western blot is a method used for detecting proteins of interest, based on antibodies' ability to bind specific antigens (proteins). Proteins are first separated with SDS-PAGE based on their size, then transferred to a membrane (nitrocellulose) by electron blotting.

30 µg of the protein sample was mixed with lysis buffer, containing SDS, and 2 µl sample buffer. The sample mix was incubated at 95°C for 5 minutes. The samples and the protein standard PageRuler were loaded into the 12% SDS-gel with 1x running buffer. Proteins were separated at 70V for 30 minutes followed by 100 V for 40 minutes.

The proteins in the gel were transferred to nitrocellulose membrane (Amersham Hybond^{TM} ECL, GE Healthcare, UK). The membrane was first soaked in MQ-water and then in 1 x-blotting buffer with 20% methanol before electron blotting.
Several different buffers were prepared for the blocking process: 10x TBS, TBS-T and TBS-T 5% milk **(appendix A.1-A.5).** The membrane was blocked with 5% non-fat dry milk (Bio-Rad, USA) in Tris buffered saline with Tween-20 (1x TBS-T) for 1 hour. The membrane was incubated with the primary antibody, rabbit anti BAX (N-20), 200 µg/ml (Santa cruz Biotechonology, USA) in 1 hour. The primary antibody was diluted in TBS-T with 5% non fat dry milk powder. After 1 hour incubation the membrane was washed in TBS-T buffer, for 3 x 5 minute, followed by incubation with the secondary antibody, Goat anti Rabbit- IgG-HRP, 1:2000 (southern biotech) for 1 hour. The secondary antibody was also diluted in 1x TBS-T with 5% non-fat dry milk. After incubation the membrane was washed in TBS-T buffer, for 3 x 5 minute. Antibody labeling was detected using visualizing kit Amersham-ECL Plus western (GE Healthcare, UK) to the manufacturer. Protein expression was quantified with syngen GelDoc.

4.7 Statistics

Statistical analysis was done using SPSS and prism 6, graphad. $P<0.05$ was accepted as statistically significant. Comparison of multiple groups was performed using one-way ANOVA. Statistically significant differences between 2 groups were tested by using the t-test. Nonparametric variables of more than 2 groups were Kruskal-Wallis test used. Statistically significance between 2 groups were tested by Mann-Whitney test. Results are given as mean or median ± SD.

5.0 Results

5.1 MTT viability tests

5.1.1 Dose-and time-dependent inhibition of cells treated with H_2O_2

We investigated the stress regions using a cell viability test applying different concentration (50,100, or 200 μM) of H_2O_2 for various time points (1 hour and 24 hours) to the cell line EFN-R.

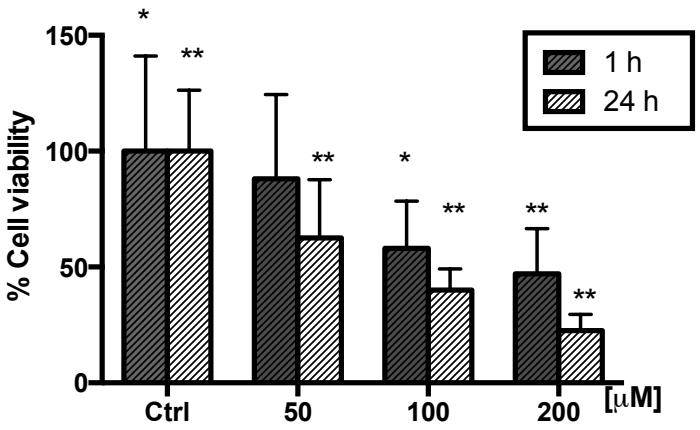

Figure 5.1: Effect of different concentration of H_2O_2 at different time points, measured by MTT assay. Cells were treated with different concentrations (50, 100, and 200 μM) of H_2O_2 and incubated either for 1 (n=8) or 24 (n=9) hours. Viable cells were assessed by MTT assay, presented in percentage compared to control for the representative time point. Values represent means ± standard derivation (SD). Statistically different values of *p<0.05, **p<0.01 were calculated with t-test and compared to cells without H_2O_2 treatment (control).

The viability of cells treated for 1 hour and 24 hours with H_2O_2 showed a linear relationship between concentration and exposure time. Cells exposed to H_2O_2 for 24 hours had a lower viability rate than cells incubated for 1 hour. Significantly difference in cell viability was observed between the control group and cells treated with 100 μM or 200 μM for 1 hour of incubation. The groups exposed for H_2O_2 for 24 hours showed a statistically significance lower viability in comparison to the control group (**figure 5.1**).

5.1.2 The effect of the potential antioxidant NACA

NACA is a protective agent against cell damage in its role as a scavenger of free radicals [106]. In order to study a potential positive effect of NACA on cell damage, it was important to find correct concentration for further experiments. Thus, the optimal concentration was tested with a viability test. Based on a concentration of 750 μM used by Penugonda et al [106].

To explore the effect of NACA, the cells were divided into two treatment groups called pre-treatment and post-treatment. Cells in pre-treatment group were incubated with 750 μM NACA for 30 minutes before exposure for 100 μM H_2O_2. Versus the cells in post-treatment were treated with NACA for 30 minutes posterior to H_2O_2 exposure. For controls, it was also tested to add 100 μM H_2O_2, 750 μM NACA or any treatment at all. All groups were incubated for 1 hour prior to assessment with MTT assay.

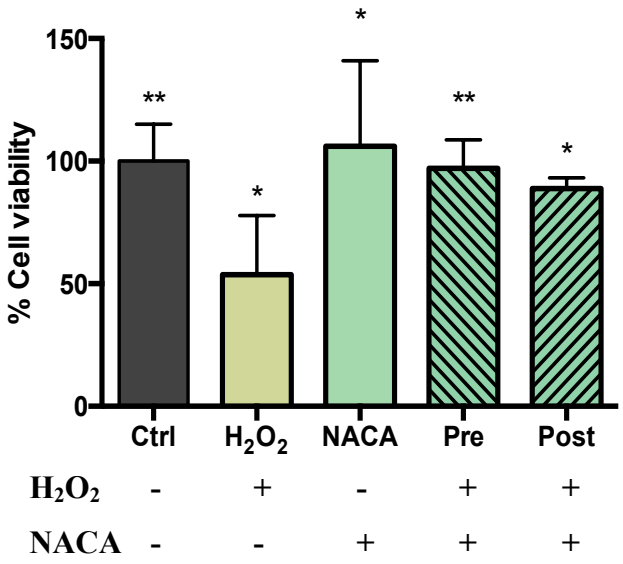

Figure 5.2: Effect of NACA on cells exposed to different concentration of H_2O_2. The cells were divided into: Control, H_2O_2, only NACA, pre-treatment or post-treatment groups. In the pre-treatment group, cells were initially exposed to 750 μM NACA for 30 minutes, and thereafter treated for H_2O_2 for 1 hour. In the post-treatment group, the cells were treated for H_2O_2 for 30 minutes before NACA-treatment and incubated for 1 hour. In addition to pre-and post treatment, the control groups were incubated for 1 hour and the viability was assessed by the MTT assay. Values represents means ± SD, and n=8. Statistically different values of *$p<0.05$ and **$p<0.01$ were calculated with t-test, compared to H_2O_2 control.

Figure 5.2 illustrate that H_2O_2 group have decreased cell viability compared to cells in the other groups. Cells treated with 750 μM NACA had a significantly higher viability than cells exposed only to H_2O_2. The EFN-R cells in both pre-treatment and post-treatment groups showed significantly difference in the viability compared to H_2O_2 group. In addition, cells in post-treatment group revealed a slightly decreased viability in comparison to pre-treatment group. There was no significant difference between the pre- and post-treatment groups. The concentration of 750 μM was used in the following experiments.

5.2 The mutation rate measured by the RMC method

A method of RMC was established to quantify DNA damage. RMC is a reliable and sensitive method to explore mtDNA and ntDNA damages, first described by Velmust et al [105], the method has further repeated by Janne et al [43]. To our knowledge, this is the first time that RMC has been tested for using pig samples exposed to hypoxia. In mtDNA the *12S* gene was tested for DNA damage and for nuclear DNA (ntDNA), we chose the *p53* gene, this due its mutation spectrum in carcinogenesis and its role as gatekeeper of the cell. The RMC method is based on the ability of damages to inhibit restriction enzyme cleavage. qRT-PCR is subsequently used to quantify amount of noncleavaged DNA template after restriction enzyme digestion.

5.2.1 Test based on restriction cleavage of DNA fragment

The samples in mtDNA digest were PCR product from EFN-R cells and cerebellum from piglets. A TaqI restriction site (TCGA) located in the gene encoding the *12S* rRNA subunit (bp 634-637) was selected for mutation frequency determination. In ntDNA the samples were genomic DNA from EFN-R cells, and the restriction site is presented in exon 3 (mutation site 175) in the *p53* gene. Restriction enzyme BfoI was selected for *p53* gene (**see appendix figure 9.1 and 9.2**) in ntDNA. The PCR product were amplified and put on 3% agarose gel (described in section 4.4.2).

(a) (b)

12S **p53**

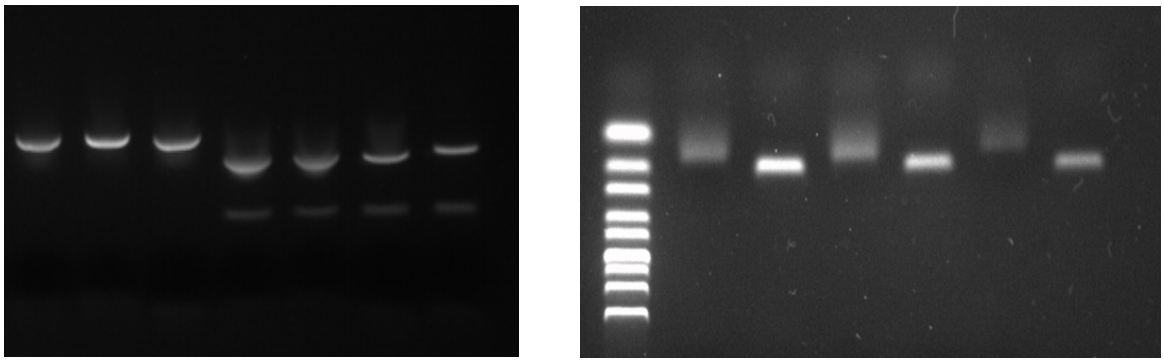

Figure 5.3: Enzyme digest with EFN-R cells and cerebellum of pigs with their representative enzyme, both in mtDNA and ntDNA, electrophoresed on 3% agarose gel. (a) Enzyme digest with TaqI with three different PCR products containing EFN-R cells and cerebellum. The first three fragments are *12S* control gene and the last four fragments are with *12S* target gene. The product size in *12S* control is 228 bp and for cleavages with TaqI, the product size are 153 bp and 70 bp. (b) The gel picture represents ntDNA treated with BfoI in *p53* gene. A 50 bp DNA ladder is shown in lane 1. The product size of *p53* is 99 bp and cleavage with BfoI, the product size are 50 bp and 49 bp, respectively.

The restriction enzyme digest of *12S* rRNA gene was quantified by qRT-PCR. PCR amplicons were subjected to restriction digest with TaqI, resulting in a single band of 228 bp due to the absence of the specific TaqI restriction site in the control gene. The target gene in presence of restriction enzyme, two bands of 153 and 70 bp were presented.

In ntDNA the fast digest enzyme was optimized with fast digest buffer. It turned out that the qRT-PCR reaction was inhibited when the enzyme and buffer was used simultaneously. Several different enzymes and digesting buffers were tested for qRT-PCR for *p53* cutting site. However, none of them were able cut in the correct restriction site. Therefore, restriction digest in nuclear DNA was performed with genomic DNA. A restriction digest was carried out, and the product was analyzed in a qRT-PCR reaction. It is difficult to distinguish between 50 bp and 48 bp. The gel picture shows the product size without cleavage at 99 bp, and the cleavage product size is approximately 50 bp.

5.2.2 Time-and dose-depended assay to evaluate oxidative stress

In order to optimize timing and concentration of potential damage accumulation in DNA, we compared mtDNA and ntDNA damages in cells treated with different concentration of H_2O_2 for various time points. We wanted to investigate whether decreased level of cell viability in EFN-R cells measured by MTT is related to the increased level of DNA damage. Initially we compared the time and dose dependent accumulation of DNA damage in the mitochondrial gene encoding *12S* rRNA, followed by testing nuclear DNA encoding *p53* gene. The oxidative DNA damages in mtDNA (*12S* rRNA) and ntDNA (*p53*) were detected by RMC (**figure 5.4 and 5.5**).

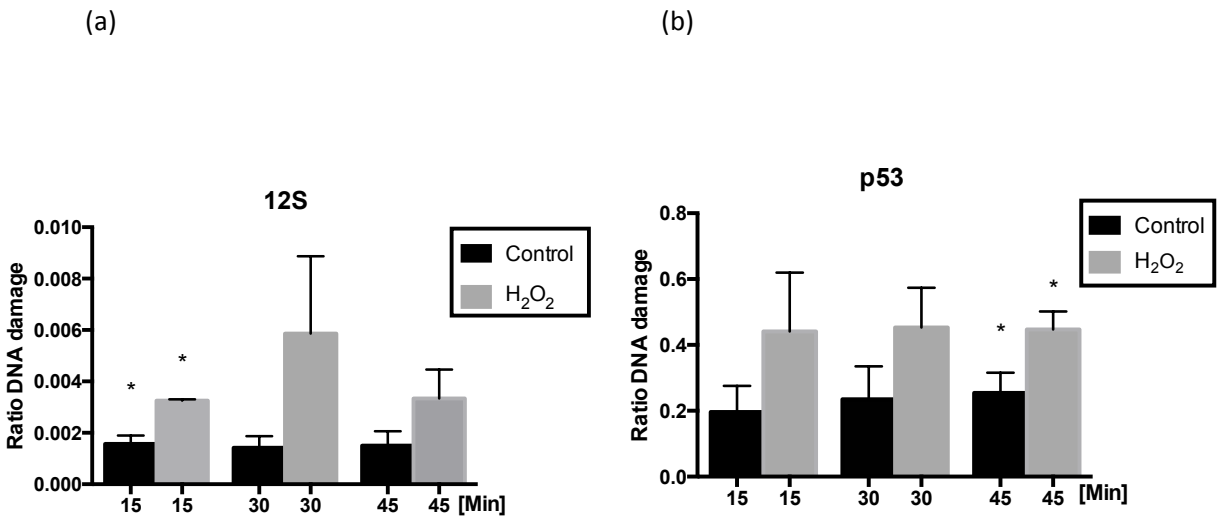

Figure 5.4: Time-dependent response curve for DNA damage using EFN-R cells: Figure (a) shows DNA damage in mtDNA. Cells were treated with 100 µM H_2O_2 for 15, 30 or 45 minutes and digested with TaqI in qRT-PCR. Figure (b) reveals DNA damage in ntDNA treated with 100 µM H_2O_2 in 15, 30 or 45 minutes and the cells were first digested with BfoI enzyme and later analyzed by qRT-PCR. Both figures are given with control group versus treatment group. Values represent means ± SD, and n=3. Statistically different values of *$p<0.05$ were calculated with t- test, compared to control.

Figure 5.4 and 5.5 exhibits the time-and dose-dependent DNA damage in both mtDNA and ntDNA. DNA damage ratio in ntDNA is 100 times higher than in mtDNA, although they show almost the same pattern. The time depend curve reveals that the control group for the different time points in mtDNA have equal ratio DNA damage. There is a significant difference in damage between the control and cells treated with 100 µM

H_2O_2 in 15 minutes. EFN-R cells exposed to H_2O_2 for 30 minutes showed an increased level of DNA damage. After 45 minutes of treatment, the DNA damage ratio decreased to almost same level as cells treated after 15 minutes. There was no significant difference in cell damage between 30 minutes and 45 minutes. On the other hand, the control group in ntDNA revealed the same tendency as in mtDNA. In contrast to mtDNA, the treatment groups in ntDNA reveals to have the same ratio of DNA damage for the different time points. Cells treated for 45 minutes, were significantly different between the control and the treatmentgroup.

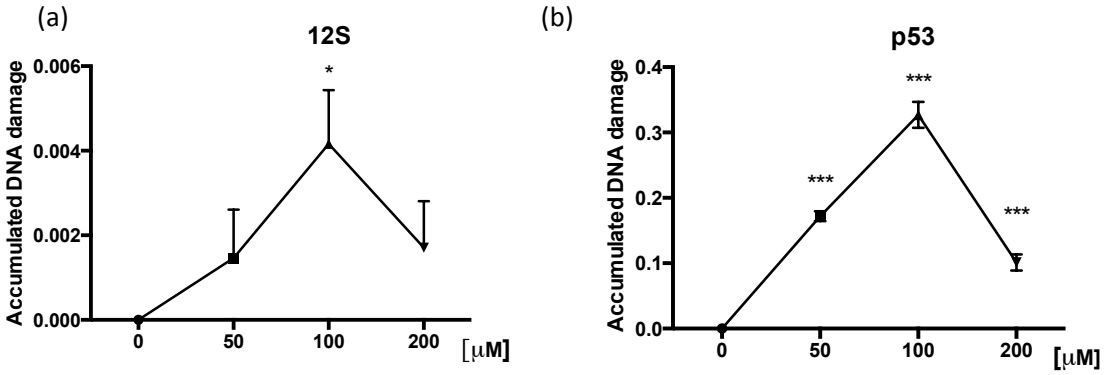

Figure 5.5: Accumulated DNA damaged level in EFN-R cells treated with different H_2O_2 concentrations. Figure a (mtDNA) and b (ntDNA) reveals DNA damage in cells treated with 50, 100, or 200 μM H_2O_2 for 30 minutes. The DNA damage was measured by RMC method, accumulated DNA where calculated relative to the control group. Data in the figure represents means ± SD of three independent experiments. *p<0.05, **p<0.01, ***p<0.001 vs. control group.

The increase in DNA damage ratio shows a linear progression until a concentration of 100 μM H_2O_2 for both mtDNA and ntDNA. For mtDNA, there is a significant difference between control group and the 100 μM H_2O_2 group. However, treatment with higher amount of H_2O_2, above 100 μM, decreased the DNA damage. The same pattern was observed in ntDNA. There was a significant difference in DNA damage in ntDNA for the three concentrations.

As shown in figure 5.4, H_2O_2-induced DNA damage had a time-depended manner with a maximum level at 30 minutes. Similarly, a dose-dependent response curve indicated an optimal damage effect for 100 μM H_2O_2 for the given exposure time (**figure 5.5**). Thus, these concentration and time point were used in following experiments.

5.2.3 Investigating the protective effect of NACA on oxidative stress

NACA are investigated as a potential treatment for neurodegeneration and other oxidation mediated disorders [106]. In order to test whether NACA protects against DNA damage, the RMC method was used to measure the DNA damage ratio. The EFN-R cells were exposed to 100 μM H_2O_2 and treated with 750 μM NACA, the cells were incubated for 30 minutes (for details see 5.1.2). There were also tested for the difference between pre treatment and post-treatment groups.

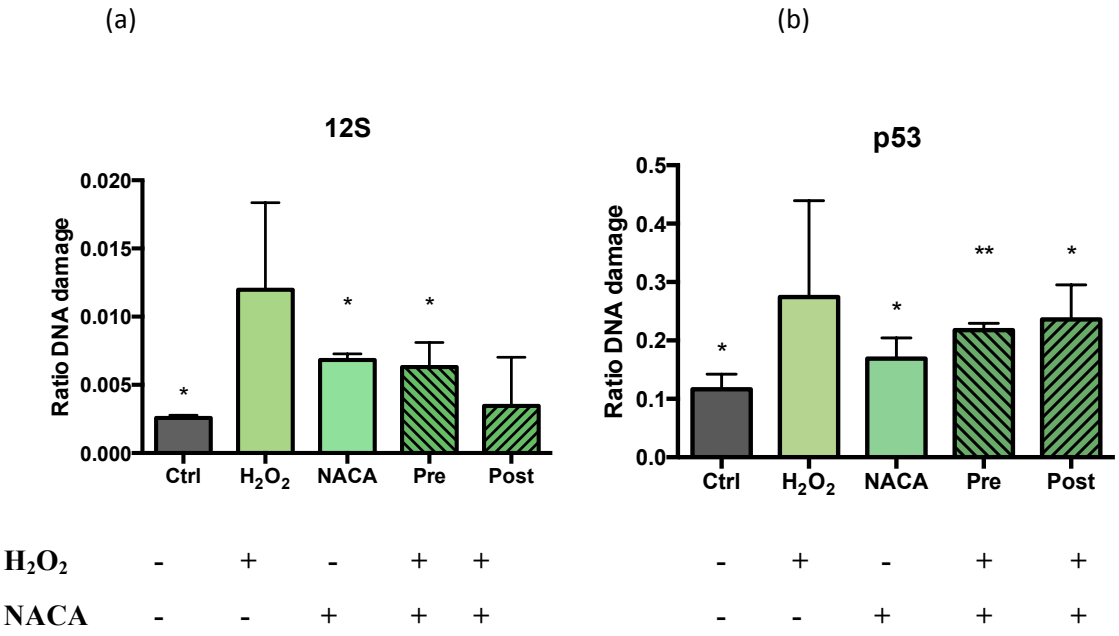

Figure 5.6: mtDNA and ntDNA damage in cells treated with NACA. The experiment was divided in to five groups and the cells were exposed to different treatments for 30 minutes. (a) Ratio of DNA damage in mtDNA. The values are given as means ± SD in 3 independent experiments. (b) Ratio of DNA damage in ntDNA, divided in: Control (n=5), H_2O_2 (n=5), NACA (n=5), pre-treatment (n=4) and treatment (n=5). Statistically different values of *p<0.05, **p<0.01 and ***p<0.001 were calculated with t-test, compared to control.

No significant differences were observed between the control- and the H_2O_2 groups in mtDNA and ntDNA. The ratio of DNA damage was highest in the H_2O_2 group, here, cells were exposed to 100 μM H_2O_2 in 30 minutes. Cells in the treatment group revealed a significant improvement in EFN-R cells compared to the control group and had a lower mutation rate than H_2O_2 group. There were no significant between treatment

groups compared to cells exposed to only H_2O_2. The post-treatment group had a lower mutation rate compared to the other groups. It was also no significance between pre- and post- treatment. The pre-treatment group showed a significant different compared to the control group and has slightly higher mutation rate than NACA group. In contrast to mtDNA, the post-treatment group in ntDNA has higher mutation ratio then both pre-treatment and NACA group.

5.2.4 mtDNA damage in cerebellum of pigs exposed to hypoxia

We used samples from cerebellum of the piglets to determine the effect hypoxia on mtDNA damage. In addition to the effect of hypoxia, mtDNA damage was also measured to investigate whether NACA had a protective effect on cell damage induced by hypoxia. DNA from cerebellum was isolated and the mtDNA damaged was measured by RMC method. In cohort I, two different hypoxia treatments were used; severe hypoxia and moderate hypoxia. Briefly, in severe hypoxia pigs were exposed to 8% O_2 until BE reached -20 mmol/l and in moderate hypoxia the pigs were exposed to 8% O_2 until BE reached -15 mmol/l. The pigs treated with NACA, received NACA immediately after hypoxia, while the non-treatment groups received saline.

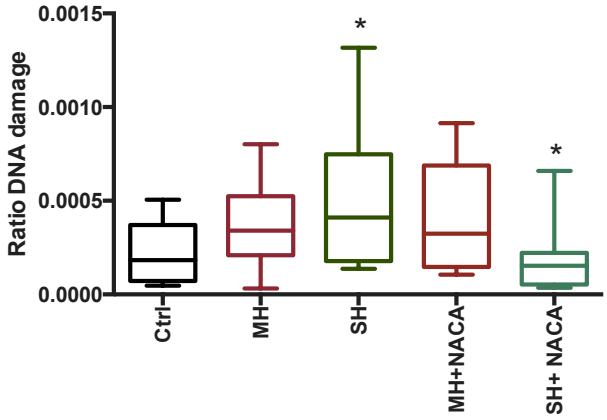

Figure 5.7: DNA damage in cerebellum. DNA damage was measured in cerebellum in pig samples from cohort 1. The samples were divided into; Control (n=6), moderate hypoxia (n=12), severe hypoxia (n=12), moderate hypoxia with NACA (n=12) and severe hypoxia with NACA (n=12). Values are given as means ± SD, and statistically different values of *$p<0.05$ were calculated by one-way ANOVA followed by t-test.

Significant differences between the severe hypoxia group versus the group of severe hypoxia with NACA was found. The hypoxia group treated with NACA has lower DNA damage than the group without NACA. Pigs exposed to hypoxia showed higher DNA damage than pigs exposed to hypoxia and later treated with NACA. For pigs without NACA treatment, the DNA damage was higher in the piglets exposed to severe hypoxia group compared to pigs treated with moderate hypoxia. NACA showed a different effect based on whether the pigs were exposed to moderate or severe hypoxia. However, we observed that DNA damages in moderate hypoxia versus moderate hypoxia treated with NACA showed an increase in opposite to severe hypoxia groups where a decrease was observed. However, no significance was shown.

5.3 Gene expression studies

In order to investigate the damage at RNA level, three pro-apoptotic genes were selected. The genes of interest were *Caspase 3*, *Bax* and *p53*. The gene expressions were analyzed by qRT-PCR in EFN-R cells treated with different concentration and exposure times of H_2O_2. The relative gene expression was normalized to the *pO* gene, and the data were analyzed to find the difference in gene expression (see 4.5.3). Figure 5.8 and 5.9 show the relative expression of genes at different concentration and time points.

5.3.1 Gene expression of cells treated with H_2O_2 for different time points

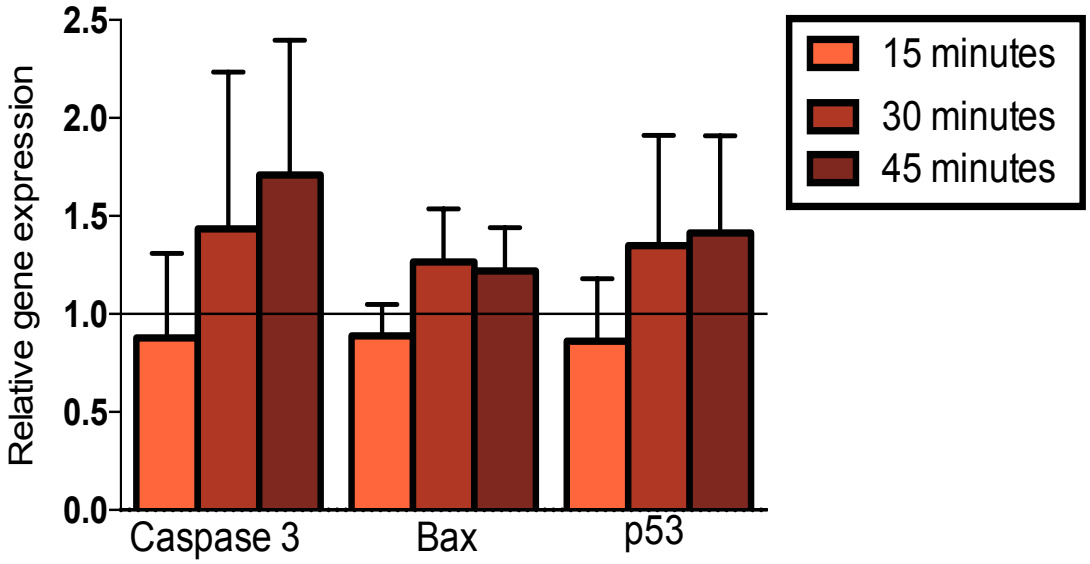

Figure 5.8: Gene expression scale at different time points. Cells were exposed to 100 µM H_2O_2 and incubated for 15, 30, or 45 minutes. RNA was isolated and the different gene (*Caspase 3*, *Bax* and *p53*) was detected by qRT-PCR as described in chapter 4.5.3. The control was calculated to 1.0. Values are given as means ± SD, of four independent experiments. Statistically difference was calculated by one-way ANOVA, and no significant differences were revealed.

The analyses of the gene expression revealed different expression in the various concentrations and time points. After 15 minutes all the investigated genes showed increase in expression. *Caspase 3* and *p53* showed higher fold change than *Bax* in cells exposed for 30 minutes. Cells exposed to H_2O_2 for 45 minutes revealed a higher expression of *Caspase 3*, while *Bax* and *p53* remains to be at same level as in 30 minutes.

5.3.2 Gene expression of cells treated with H_2O_2 for various concentrations

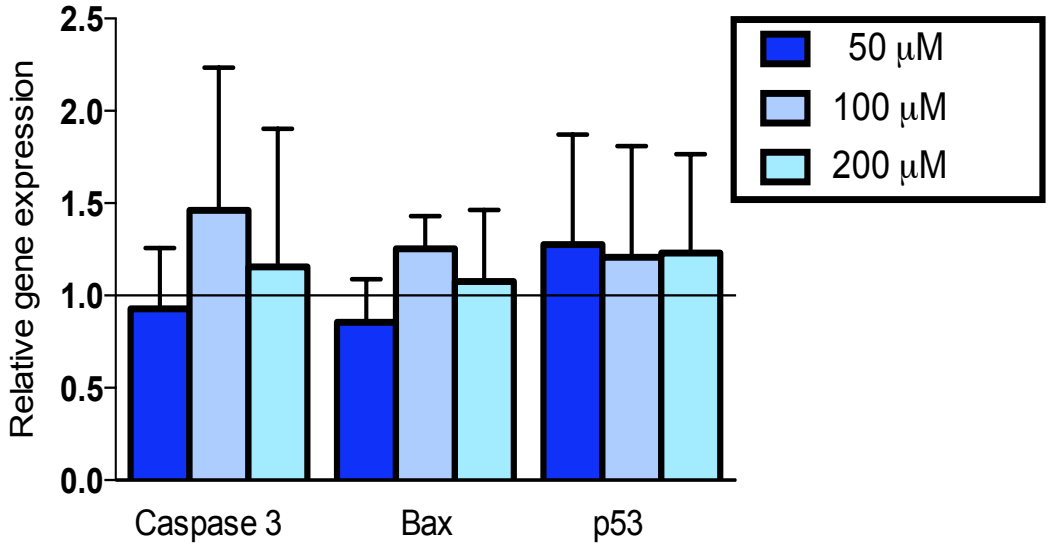

Figure 5.9: Gene expression in dose depended curve. Cells were exposed 50, 100, or 200 µM H_2O_2 for 30 minutes. RNA was isolated and quantified in qRT-PCR as described in chapter 3.3 Gene of interest was *caspase 3, Bax* and *p53*. The control was calculated to 1.0. Values are given as means ± SD, of four independent experiments. Statistically difference were calculated one-way ANOVA, and no significant differences was showed.

Different concentrations of H_2O_2 were examined, and the cells treated with 50 µM H_2O_2 revealed a lower fold change in *Caspase 3* and *Bax*. The expression of *p53* was higher compared to *Caspase 3* and *Bax*. In 100 µM H_2O_2 are all three genes up-regulated, *Caspase 3* have higher fold change compared to the other genes. *Bax* and *p53* were up-regulated at same level. After stress induced with 200 µM were the genes lower expressed than in 100 µM. The *p53* have the same fold change in 200 µM H_2O_2, as in 100 µM H_2O_2. *Caspase 3* and *Bax* have lower fold-change in 200 µM H_2O_2 stress.

5.3.3 Effect of NACA at mRNA level

The potential protective effect of NACA to oxidative stress was investigated on the mRNA levels. EFN-R cells were treated differently in four groups as described in chapter 5.1.2 and the relative gene expression was normalized to the *pO* gene, and the data were analyzed to find the difference in gene expression.

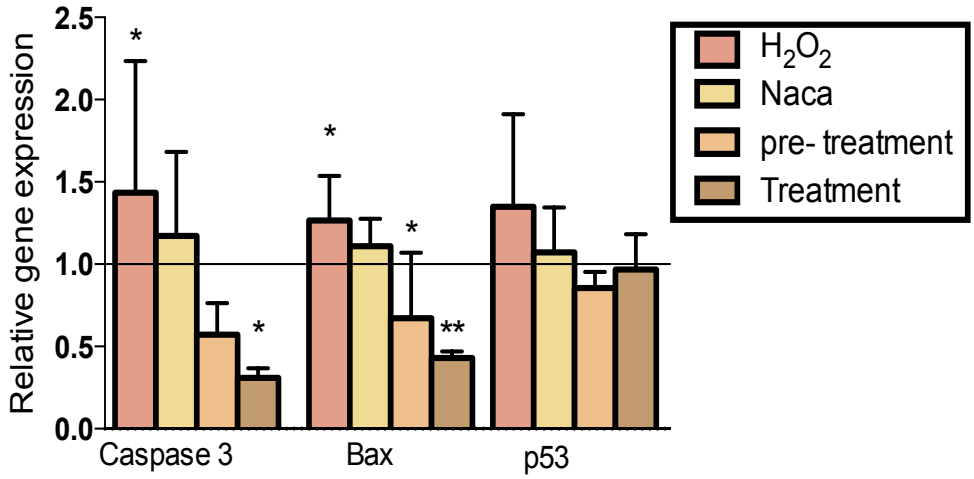

Figure 5.10: Gene expression of cells treated with NACA: Cells were divided in different groups: control-H_2O_2, control-NACA, pre-treatment and post-treatment. In pre-treatment were cells treated with 750 µM NACA for 30 minutes before exposure of 100 µM H_2O_2. In post-treatment were cells exposed to 100 µM H_2O_2 for 30 minutes prior to treatment with 750 µM NACA. The control group were exposed to either 100 µM H_2O_2 or 750 µM NACA for 30 minutes Values are given as means ± SD, of four independent experiments. Statistically different values of p* <0.05 and p* < 0.01 were calculated with one way ANOVA, followed by t-test.

Cells exposed to 100 µM H_2O_2 were highest expressed of the four groups. *Caspase 3* showed a significant difference between H_2O_2 compared to post-treatment groups. The expressions of *p53*, *Bax* and *Caspase 3* in pre- and post-treatment groups were lower than the other groups. No significant differences between the two treatment groups were observed. In *Bax* a similar pattern was revealed. Both, pre- and post treatment exhibited significance differences compared to H_2O_2. *p53* gene, which involves controlling apoptosis, were expressed differently compared to the two other genes. Expression of *p53* has a higher fold change in treatment group compared to *Caspase 3* and *Bax*. Nevertheless no significant differences were revealed in p53. Cells only exposed to NACA showed same level of expression in *Caspase 3*, *Bax* and *p53*.

5.4 Protein expression

To investigate the damages found at the DNA and RNA levels, we tested further with protein expression. DNA damage can leads to apoptosis and one of the key players in apoptosis is BAX. BAX promotes apoptosis induced by removal of growth factors and other stimuli [68, 105]. To confirm the expression of BAX, growth factors were removed and cells were induced with H_2O_2. Cells were exposed to 100 µM H_2O_2 for different time points: 45 minutes, 90 minutes, 3 hours or 18 hours (**figure 5.11**). Jurkat cells lack BAX and consequently used as negative control. In addition to negative test, β-actin was used as control for the western blot analysis.

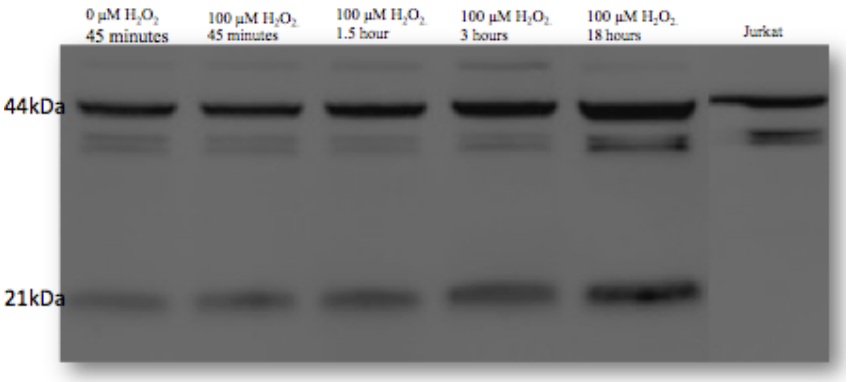

Figure 5.11: Western blot analysis of BAX in EFN-R cells induced with H_2O_2. EFN-R cells were treated with 100 µM H_2O_2 for different time points (45 minutes, 90 minutes, 3 or 18 hours). As negative control Jurkat cells was used. β-actin was used as housekeeping protein with a band size of 42 kDa. BAX was present with a band size of 21 kDA, at all four time points, with increasing stage.

As displayed in figure 5.11, expression of BAX increased proportionally with longer incubation time. After 18 hours the fragment strength were higher than other time points. BAX is represented in all time points with a band size of 42 kDA. The expression of BAX showed to be higher in longer incubation. The figure also shows that BAX expression lack in Jurkat cells, and the negative control worked.

5.5 Quantitation of cfDNA

cfDNA is on its way to become established as a non-invasive cancer biomarker. In addition to cancer, increased level of cfDNA is also reported in conditions such as stroke and trauma. It is convincing that neonatal asphyxia and cancer share similar pathogenesis, including cell death. Thus, cfDNA may also be used as biomarker in neonatal asphyxia. To our knowledge, cfDNA in pig models has not been previously investigated. Therefore, methodical adaptions were a requirement to investigate cfDNA of pig samples.

5.5.1 Evaluation of various cfDNA extraction methods

In order to find the optical extraction method for cfDNA in piglets, several DNA extraction kits were compared, concerning the DNA recovery rate and the DNA final concentrations measured in eluated of identical samples **(table 5.1).** Three different kits were tested and the average DNA concentration, purity, volume, and handling time were evaluated. Extraction kits that we tested were: Dneasy Blood & Tissue kit (Qiagen), Nucleospin plasma (Macherey & Nagel) and Wizard genomic DNA purification kit (Promega). Qiagen kit and MN-kit are both silica membrane-binding kits, and are a lot similar to each other. In other hand, Wizard kit is a salt and isopropanol precipitation based method.

Table 5.1: Comparison of cfDNA extraction efficiency, DNA quality and handling time by three different extraction methods. Three different samples with parallels were analyzed. Average DNA concentration, OD ratio was calculated as described in section 4.2.3. The handling time was calculated for 20 prepartions.

Sample	Extraction method	Kit	Company	Average DNA concentration	OD ratio 260/280	Handling time (20 preps)
Plasma	Silica membrane binding	DNeasy Blood & Tissue	Qiagen	2.35ng/µl	1.73	1.0h
Plasma	Silica membrane binding	Nucleospin plasma	Macherey & Nagel	3.23ng/ µl	2.64	1.5h
Plasma	Salt and isopropanol precipitation	Wizard® Genomic DNA purification kit	Promega	75.06ng/ µl	0.86	2.0h

Different initial volumes were tested to yield higher DNA volume. The results show that there was no difference in yield starting sample volumes of 220 µl or 440 µl. Thus we choose 200 µl for our further experiment. In addition, full blood was also investigated. The results showed a higher concentration of cfDNA in plasma samples (results not shown).

The three extraction methods showed remarkable difference in the yield of DNA from blood plasma. In MN-kit, ethanol was added to washing buffer and the last incubation step was at 90 °C. Thus, it was difficult to the small amount of eluate for further treatment. In the Wizard kit, the last step dissolving the pellet was difficult, even after intensive heat treatment over time.

Although, MN-kit gave quite similar results in yield plasma as the Qiagen kit, the sample was eluated only in 40 µl, while Qiagen was eluated in 100 µl. The DNA purity given in OD ratio 260/280 was slightly too high in MN-kit. In our hands, Qiagen kit turned out to be the best-suited method for our purpose.

5.5.2 Recovery test

Three different methods for our application were tested in order to investigate the recovery of the DNA isolation with Qiagen method (see 4.3.1). We used test sample from pig plasma spiked with 100 ng/µl DNA standard from porcine. We found a recovery of 30-40%. In other hand 40-50% recovery was found in the sample spiked with 100 ng/µl DNA standard from human male. Finally we used DNase to determine grade of DNA degradation and approximately 70-80% of the DNA was degraded.

5.5.3 Standard curve

We tested different standards to estimate the cfDNA concentration in photometric measurement and qRT-PCR. Commercial salmon sperm was first tested, as proposed in Goldenstein et al [101]. This proved to be difficult because of two reasons. The salmon sperm powder was difficult to resolve in PBS, and the standard curve was not linear. In addition to commercial salmon sperm, we tested human male DNA. The standard curve for human male DNA was acceptable to use for measuring cfDNA. Because we used samples from piglets it was more desired to use DNA from pigs. We tested therefore standard from porcine DNA. The concentration of DNA in the standard curve ranged from 0 – 1250 ng/µl. Both, for DNA standard with human male and for porcine DNA, were the standard curve linear up to 1250 ng/µl. Standard was measured photometric with SYBR® gold and with qRT-PCR (**figure 5.13**), as described in section 4.3.2.

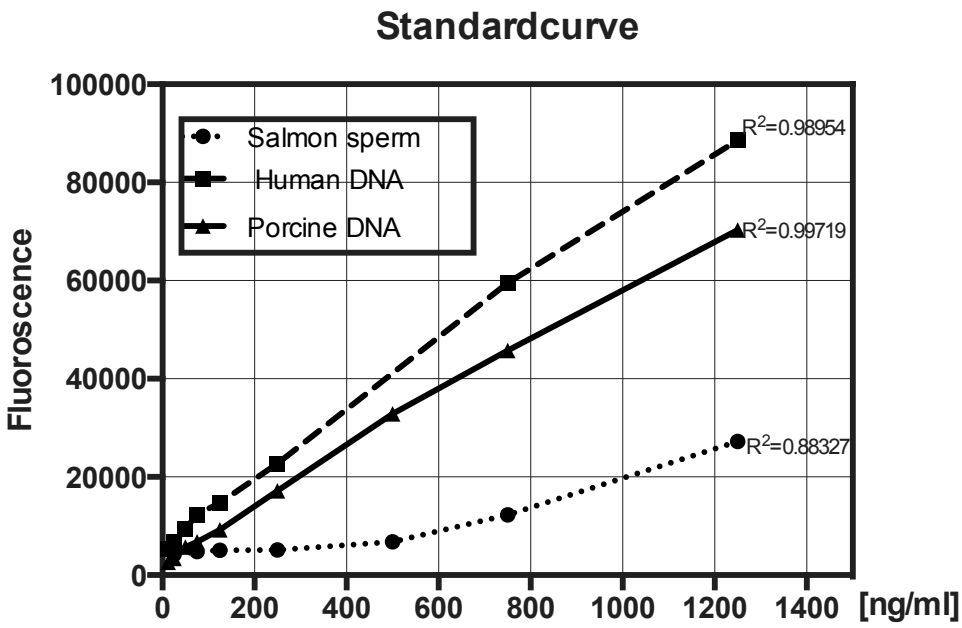

Figure 5.13a: Comparison of different standards for measuring cfDNA in blood plasma. Standard were measured photometric with SYBR® gold. DNA solutions were added in duplicates to black 96 well plates, SYBR® gold was added to each well (1:10.000) and fluorescence was measured by a plate reader fluorometer (Perkin Elmer, Viktor). The dilutions were measured in parallels.

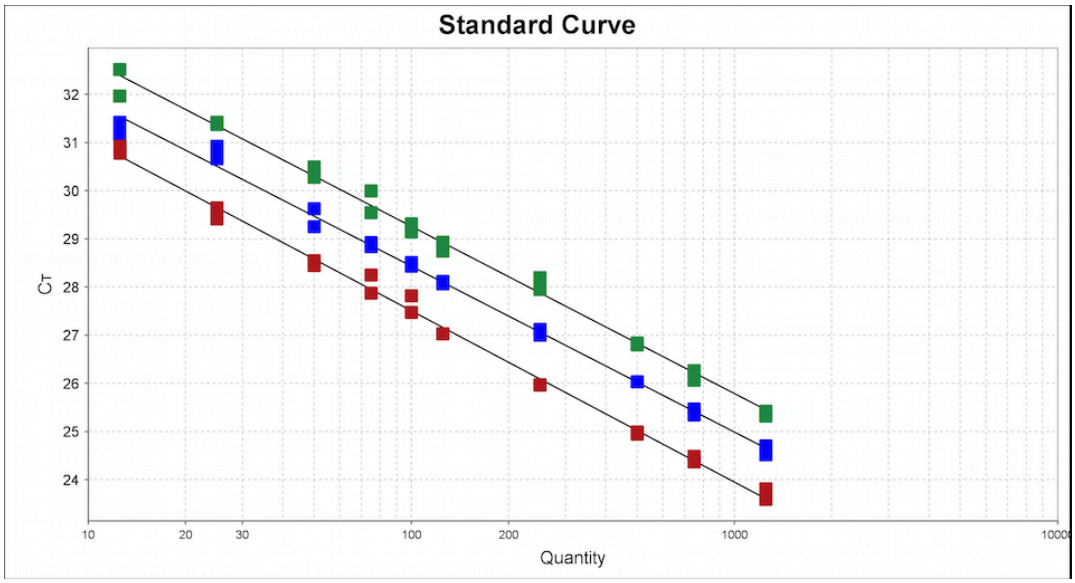

Figure 5.13b: Comparison of fragmented standard measured by qRT-PCR. Standard were measured by HMBS gene in qRT-PCR. The DNA was fragmented with two different methods. (1) DNA fragmentation with restriction enzyme, (2) DNA standard without fragmentation, (3) DNA fragmentation with UV-bath.

5.6 Methods to quantify cfDNA

Different techniques have been used to measure concentration of cfDNA in blood and tissue samples. In literature both qRT-PCR and photometric method have been used to investigate cfDNA. We wanted to test both methods for our purpose, and estimate if there is a significant difference between the methods.

5.6.1 cfDNA measured by photometric methods

In order to investigate the difference in cfDNA concentration in human and piglets, we tested cfDNA in plasma from an adult human and an adult pig. The concentration was measured by photometric method using SYBR®gold. In addition to cfDNA in human, it was also desirable to measure the difference between adult pig and newborn pig, since we used newborn pigs in our study.

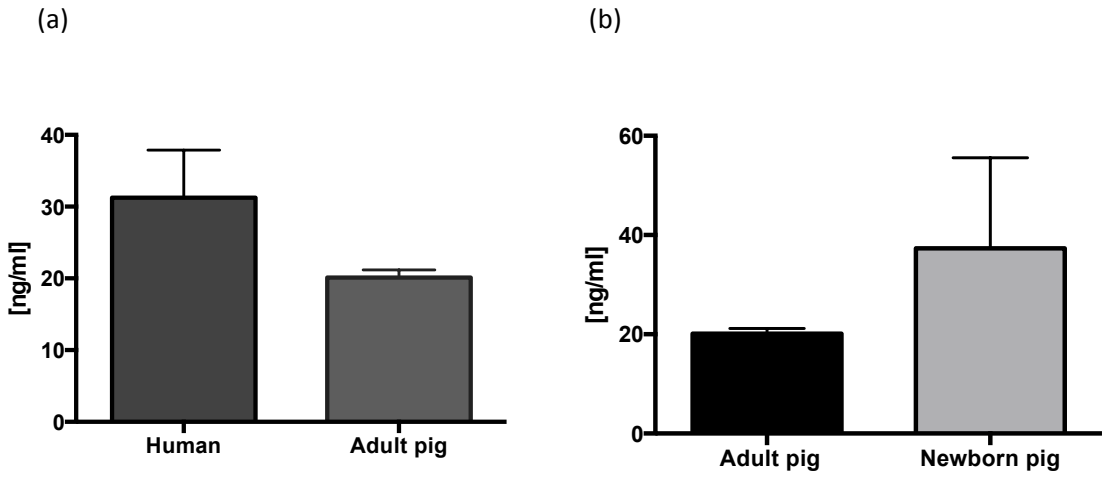

Figure 5.14: Distribution of cfDNA in humans and pigs blood plasma. Concentration was measured by photometric method with SYBR® gold. Three independent samples were measured with duplicates. Figure (a) shows concentration in human versus adult pig. Figure (b) shows adult versus newborn pig. Results are given in means ± SD and no statically significant were shown.

The plasma sample used in this purpose, were collected from healthy individuals. cfDNA in human blood plasma had a mean concentration around 30 ng/ml and in adult pig around 20 ng/ml (**figure 5.14a**). However, the comparison between adult pigs and

newborns shows that concentrations of cfDNA in newborn pigs were twice as high in adult pig (**figure 5.14 b**).

5.6.2 Photometric measurement of cfDNA in pigs treated with hypoxia, NACA and hypothermia

Two independent cohorts were used to measure the concentration of cfDNA in blood plasma from piglets. Both control and hypoxia group are presented in cohort I and cohort II. The last group in the cohort involves different treatments. In cohort I were the pigs treated with NACA and in cohort 2 were the pigs exposed to hypothermia. Briefly, the piglets were exposed to hypoxia until BE reached -20 mmol/l (see 3.2) and immediately treated with either NACA (cohort I) or hypothermia (cohort II) and reoxygenated for 30, 240, and 540 minutes after hypoxia treatment. For the non-treatment group, saline was given immediately after exposure.

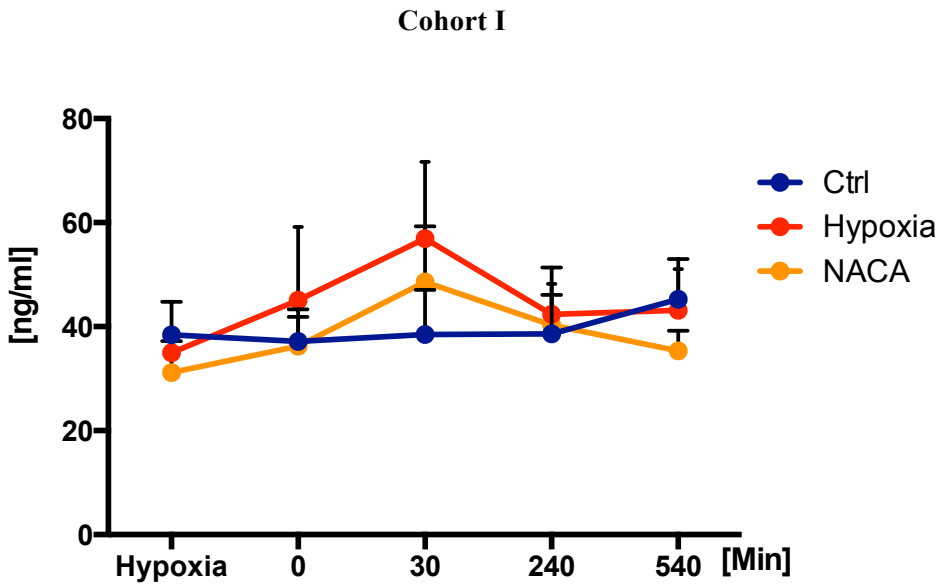

Figure 5.15a: cfDNA concentration measured by fluorometric with SYBR® Gold in cohort 1. The concentration cfDNA were measured in control group (n =5), hypoxia group (n=10) and NACA group (n=6). Results are given in means ± SD and measured in duplicates. Significant difference was calculated with ANOVA, however no significance was revealed.

Cohort II

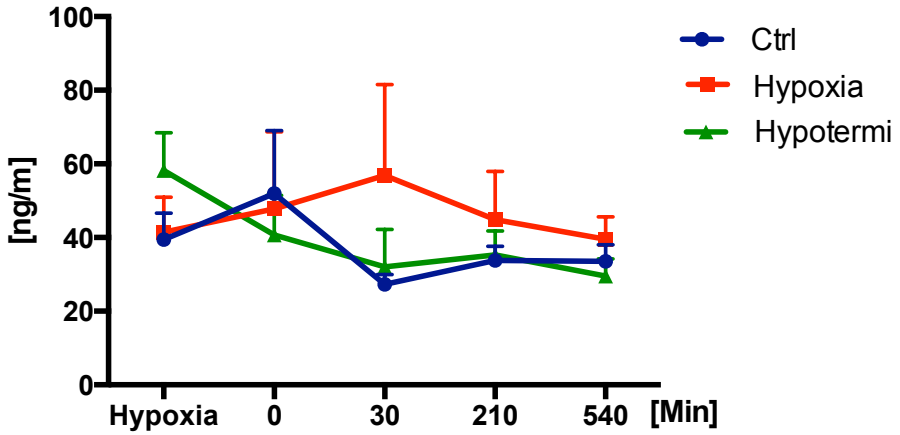

Figure 5.15b: cfDNA concentration measured by fluorometric with SYBR® Gold in cohort 2. Groups used in cohort 2 were control group (n=6), hypoxia group (n=10) and hypothermia group (n=10). Results are given in means ± SD and measured in duplicates. Significant difference was calculated with ANOVA, however no significance was showed.

Pigs exposed to hypoxia until 30 minutes reoxygenation (**figure 5.15b**) has an increased concentration of cfDNA. The figure shows a peak of cfDNA at this time point. After 30 minutes the cfDNA concentration in hypoxia group decreases. In NACA group in cohort 1, the curve shows similar changes as in the hypoxia group, although concentration of cfDNA was lower than the hypoxia group. The cfDNA level in the control pigs reveals frequently changes. Control group in cohort II shows a slightly increase in concentration after reoxygenation and afterwards decrease and stabilize after 30 minutes. The hypoxia group showed same pattern as hypoxia group in cohort I. Pigs exposed to hypothermia had a higher start concentration than the other groups, and afterward it decrease to the same level as control group.

5.6.3 cfDNA measured by qRT-PCR

In addition to photometric measurement, qRT-PCR were tested to measure the cfDNA concentration. In this method several different target genes (HMBS, PMM1, β-globulin) were used. The gene that showed highest concentration of cfDNA was β-globulin. Figure 5.16 reveals the concentration of cfDNA in hypoxia increases, and has a peek at 30 minutes, while the concentration in the control group showed few changes.

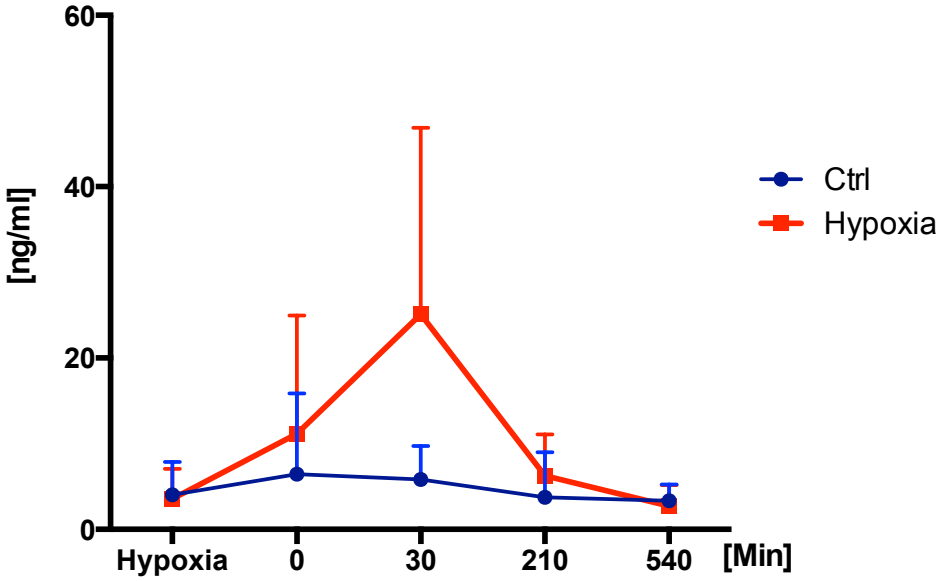

Figure 5.16: cfDNA measured by qRT-PCR with β-globulin gene. The plasma samples used in qRT-PCR measurement were control (n=6) and hypoxia group (n=12) from cohort 2. Results are given in means ± SD and measured in duplicates. Significant difference was calculated with ANOVA. However, significance was not revealed.

5.6.6 cfDNA in CSF

In addition to cfDNA in blood plasma, we tested concentration of cfDNA in CSF from piglets in cohort 1. Piglets were exposed to different levels of hypoxia and NACA treatment (see 3.2). CSF was collected 540 minutes after the reoxygenation. cfDNA was measured by photometric method with SYBR® gold.

Significant difference in concentration of cfDNA was observed between moderate hypoxia and the piglets exposed with moderate hypoxia and later treated with NACA. In figure 5.17 was observed higher concentration of cfDNA in the groups treated with

NACA, compared with groups exposed only to hypoxia. The control group has a concentration at same level as in severe hypoxia.

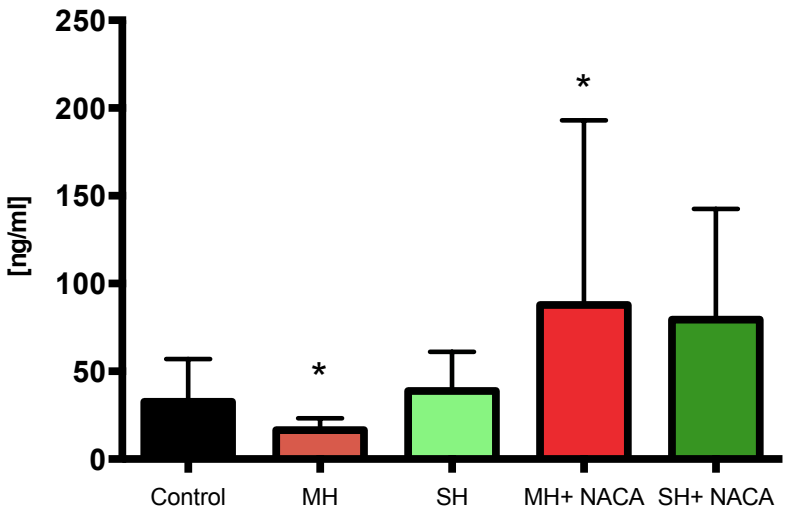

Figure 5.17: cfDNA in CSF measured fluorometric with SYBR® Gold. Control (n=5), moderate hypoxia (n=5), severe hypoxia (n=10), moderate hypoxia with NACA (n=5) and severe hypoxia with NACA (n=6). Significant difference calculated with ANOVA between values control group and the other groups and between moderate hypoxia with and without NACA, severe hypoxia with and without NACA.

6.0 Discussion

Birth asphyxia is a severe medical issue and there is therefore a high demand to develop biomarker that can help to estimate the damage after an event of asphyxia. In this thesis, we used cell lines and newborn pigs to study different independent biomarkers for measuring the degree of damage after exposure to ROS. Our aim was to develop a reliable and rapid method to measure oxidative damage. We tested cfDNA and RMC to measure the damage occurring after oxidative stress during asphyxia.

6.1 Estimating DNA damage

ROS can lead to DNA damage, which can stimulate mutation and lead to inheritable diseases like cancer [23]. In the literature, it is suggested that induction of apoptosis would lead to greater damage [43]. To find optimal reaction spectra in order to test the mutation ratio, we first had to find a concentration of H_2O_2 and time point. The MTT assay was used to test different concentration and time points of H_2O_2 treated EFN-R cells. Various concentrations and time points were chosen, based on Janne et al [43]. H_2O_2 is a well-known stress medium, readily available and easy to handle. Other researchers have also used menadione or UV radiation as stress. These provide an increased damage and give us both single- and double-stranded break [43]. A decreased cell viability after 24 hours incubation in stress medium was observed applying MTT assay, leading to cell death. Cells incubated for 1 hour with 100 μM H_2O_2, revealed cell viability at approximately 50%, therefore 100 μM H_2O_2 was chosen to use in further experiments.

6.1.1 Establishing RMC method

Spontaneous mutation are rare events that occur randomly throughout the gene, and RMC method was chosen to detect those spontaneous mutations and to measure H_2O_2 induced cell damage. The method is based on one specific mutations in the selected target gene and how frequently this mutations occurs. The RMC method was primarily established to estimate mutation ratio in mtDNA. In our study we investigated this

further with ntDNA. This allowed us to estimate the difference in mutation rate between mtDNA and ntDNA. The protocols for this method required adaptions for both mtDNA and ntDNA, including novel prior fitting to pig DNA and designing novel primers. For ntDNA the protocol had to be improved, because the original enzyme was optimized with the fast digest buffer. When this was applied together in a qRT-PCR, the reaction with the master mix was incompatible. We therefore ended up to run two separate reactions. First an enzyme digest reaction was performed, thereafter the digested product was analyzed in qRT-PCR.

The advantages of RMC method are technical simplicity, effectiveness and the fact that it does not require many resources. The method can be applied to both cells and tissue samples. Crucial for this method however, is that the input amount has to be equal for all samples. In addition, the samples should be analyzed relatively quickly after isolation. Halsne et al [52] showed that the storage of samples over time might affect the mutation rate. Another disadvantage could be that the damages may induce changes in conformation and the restriction cleavage may be positioned outside the palindromic recognition sequence. The region of the damage may span wider than the recognition sequence off restriction enzyme.

6.1.2 DNA damage measured by RMC method

To investigate DNA damage, we first made a time and dose-response test. After 30 minutes of stress, we observed increased damage in mtDNA followed by a decreasing damage after 45 minutes. Therefore we propose that the repair mechanism starts between 30 and 45 minutes. A similar pattern is observed of Janne et al [43], where the repair mechanism started after 60 minutes. The differences between the two studies may be use of various stress factors, concentrations and cell types.

An important result is that control samples are almost identical in the different time points. This may indicate a continuously natural background damage level. The cells from the control group are more stable than cells exposed to stress. In mtDNA damage induced by different concentration of H_2O_2 (**figure 5.7**) shows that there is a higher damage in 100 μM stress compared with 200 μM. The decrease might be explained by cell death. Same observations have been revealed of Janne et al [43].

In the time-response curve the damage is similar for different time points. This may indicate that the time from 15 to 45 minutes after hypoxia propose a lower value, when detecting damage of ntDNA. There may be a tendency for steady state, where the damages represent the balance between formation and repair. The repair mechanism in mtDNA is more frequent than in ntDNA. A previous study demonstrated that repair of induced damage is efficient with the major exception being repair of mtDNA, which is delayed and slower compared to repair of ntDNA [43]. This may also be explained by lower frequencies of cell division in ntDNA than in mtDNA. In addition we see the same observation with 200 μM H_2O_2 in ntDNA as observed in mtDNA. We may conclude that cell death also involves in the reaction.

6.1.3 mtDNA versus ntDNA

It is known that mtDNA is more prone to ROS-induced DNA damage than ntDNA, probably due to the close proximity to the site of ROS production in the mitochondria and different organization of DNA [43]. There are also 1000 times more mtDNA than ntDNA in cells [48]. We were expected to observe a higher mutation ratio in mtDNA in comparison to ntDNA. However, the opposite was found. We got 100 times higher mutation ratio in ntDNA. An explanation for this unexpected result might be that *p53* is frequently mutated in cancer, and have a mutation hotspot and therefore has a higher mutation ratio. The *p53* gene was chosen because of its predominant role in cancer, and known as a highly mutated gene in apoptosis [107]. On the other hand, it may be a higher mutation frequency in *p53* gene compared to *12S* gene. The *12S* gene was chosen because it was already established and got reliable results in Vermulst et al [105].

Vermulst et al [105] reported that TaqI sites at different positions displayed similar mutation characteristics with respect to frequency, age-dependence, and type of mutations. We can not rule out that the mutation site in pigs has the same mutation, but the total mutation rate remains similar. However, the restriction site in p53 is not studied further. A limitation of our study is that we did not test other sites in p53 to confirm a generally higher mutation ratio in ntDNA compared to mtDNA.

6.1.4 NACA as a protective antioxidant

As proposed in Penugonda et al [106], we used 750 μM NACA for our experiments. In their present work, they have found a protective effect of NACA with glutamate as stress agent. In order to test NACAs protective effect further, we tested the effect before or after stress in two different groups; pre-and post treatments. However, the difference between the groups was not detectable. Nevertheless, our data on cell viability correlated with the observations in article of Penugonda et al [106] where NACA did show a protective effect.

To investigate the effect of NACA, both mtDNA and ntDNA were used. Our results showed that NACA had a protective effect. To our knowledge there is no literature proving NACAs effect directly on DNA damage. Although Penugonda et al [106] showed that NACA has a protective effect, regarding cell viability. The results show a significant reduction in the ratio of DNA damage in both pre- and post-treatment in mtDNA. When administered before treatment, NACA only had a protective effect regarding DNA damage on ntDNA. Our results are in line with other publications highlighting a protective effect of NACA in oxidative stress situations [78]. Although, we revealed a difference between pre and post-treatment, but there is no significance. Therefore it is difficult to say whether is random or there is a difference inducements in ntDNA and mtDNA. In addition we also observed a higher effect of NACA in mtDNA compared to ntDNA. This can truly be explained by NACAs higher permeability through mitochondrial membranes [78].

6.1.5 DNA damage in pigs exposed to hypoxia

The mutation ratio in cerebellum from pigs exposed to hypoxia were measured by the RMC method. After exposure of either moderate or severe hypoxia, the pigs were treated with NACA or saline. There was a tendency of increased damage for the pigs exposed to severe hypoxia compared to moderate hypoxia. Our hypothesis was that NACA protect against DNA damage. This was confirmed by a significant higher degree of damage for pigs receiving saline after severe hypoxia than pigs receiving NACA. We propose that NACA has not only an effect on EFN-R cells, but also in cerebellum of the pigs. One thing that stands out from our hypothesis is that the group receiving NACA after moderate hypoxia has an opposite effect. It might be the case that in moderate

hypoxia the damage is not sufficiently enough, and therefore the NACA has an opposite effect.

6.1.6 Expression in mRNA and protein level

To confirm our hypothesis that we get a higher damage by increased stress, we investigated the protein expression BAX. Our results were in line with the hypothesis. The expression was also used to confirm the mRNA expression.

Different genes are used as biomarkers for measuring oxidative stress to relate our results on the DNA levels. We further investigated expression of proapoptotic genes after higher levels of oxidative stress. Genes of interest were selected with respect to their expression during apoptosis. *p53* is a pro-apoptotic gene that is up-regulated during apoptosis. Our results showed that *p53*, *Bax* and *Caspase 3* are up-regulated after 30 minutes in 100 μM H_2O_2 exposure. Hence, we can conclude that the oxidative stress induced apoptosis and our biomarker revealed a similar pattern as the gene expression. *Caspase 3*, *Bax* and *p53* are three different genes together in a cascade. These genes are not consecutive and are independent. Nevertheless, we see a gene expression in all three genes. This confirms that a stress response has been induced over time. In addition, NACA showed an impact on pro-apoptotic genes *Caspase 3* and *Bax*, where the genes are down-regulated in pre-and post-treatment groups. NACA did not influence the gene expression of *p53*.

6.2 Quantitation of cfDNA as novel biomarker

In the last decades, numerous papers have repoted that the quantification of cfDNA in plasma and serum might be a promising biomarker in many pathological conditions [94]. There is still uncertain how cfDNA are released. Some authors [71, 81] claim that cfDNA is only released from apoptotic cell, other state that it may be generated by both, apoptotic and necrotic cells. The concentration of cfDNA in circulating blood has shown to be substantially affected by the blood sampling and blood processing protocols. Large amounts of alternative protocols for isolating cfDNA from body fluids including plasma, serum, urine, and CSF have been presented [81]. Various extraction methods based on columns or magnetic beads have been tested for extraction of cfDNA.

In addition, different detections methods like qRT-PCR and photometric measurements have been established [86]. However, there is an ongoing debate about the optical methods for extraction as well as measuring the quantity.

Three different kits MN-kit, Wizard kit and Qiagen Blood and Tissue kit were tested, and the latter turned out to be the most suitable extraction method for our purposes. However, we are aware of that several further methods are available. Qiagen kit is frequently used for extraction of cfDNA in several literatures, and in our study the kit turned out to be a rapid and reliable method. In a comparison, a protocol done by DNA Bank network [108], the Dneasy Blood & Tissue Kit (Qiagen) was preferred for animal samples. The test results shown in the protocol were in line with our results. A disadvantage however, might be the loss of the small fragments due to the column. In the future, the samples that we have tested so far should also be tested with King Fisher Duo, which is based on magnetic beads. Then, the difference between column-based extraction and magnetic beads can be determined.

6.2.1 Measurement of cfDNA

The concentration of cfDNA tends to vary among healthy individuals. The large variation in measured concentration can be explained by the use of different protocols for blood processing, as well as the time difference between blood drawing and separation. On the other hand, different methods for extraction and detection might have an influence of the high variability of the concentrations of the different samples. The reference area for cfDNA is wide in most literature, for instance in Gormally et al [83] the concentration vary from 0-100 ng/ml with an average of 30 ng/ml. Our measurements had an average of 30 ng/ml, similar to Gormally et al [83]. Because of the uncertainties surrounding the references values, comparing our results to other studies is complicated.

Our results show that adult pigs have a lower cfDNA content compared to newborn pigs. This is in line with the human study shown in Tuavea et al [87]. The results implicate that pigs revealed lower concentration of cfDNA compared to humans. This point should be taken into considerations when use of pigs in cfDNA studies. In our knowledge, concentration of cfDNA in other animals has not been measured.

The only method used to measure cfDNA in human and adult pig plasma was fluorescence. Ideally, qRT-PCR should have been used to confirm the results. Comparing human and pig sample with qRT-PCR however, this requires primers designed for the same sequence in human and pigs.

6.2.2 Photometric versus qRT-PCR methods

There have been a number of tests done for detection of cfDNA, and many different methods have been studied [95, 109]. We investigated the difference between the photometric and qRT-PCR. Both methods have been tested and described in different literatures [86, 91]. The methods required a good standard curve to measure the concentration of cfDNA. Hence, we tested different standard including male DNA, porcine DNA and salmon sperm. Small differences in male DNA and porcine DNA were observed. This might be affected by different extraction method used to gain DNA, as well as use of different buffers. However, salmon sperm DNA was difficult to dissolve as it was in powder. Thus, we did not reveal a good standard curve. Our results exhibited that standard curve with porcine DNA was more suitable for our purpose. Because cfDNA contains small fragments, there were also done different fragment tests. Nevertheless, the results did not show any difference with the fragmented standard.

Photometric method is often referred as a nonspecific method, because measurements with this method not only bind specific to our product, but also other nucleic acids, small fragments etc. In the other hand, qRT-PCR is a more accurate and highly sensitive technique used in molecular biology. This is because it only determines a defined area in the gene. For the photometric method, a detection dye called SYBR®gold was chosen. This is a sensitive flurophore available for detecting single-or double-stranded RNA or DNA [101]. Numerous other detection dyes are available. The detection limit and sensitivity is proved to be better in SYBR®gold [101]. The disadvantage with the photometric method is to distinguish between the background noise and the results. qRT-PCR proves to be more specific. In this method the challenge was to find a gene to measure the cfDNA. In the literature, different genes have been tested. In our case it was the first time pigs have been used in this kind of study. Therefore we had to design new primers. It turned out that different genes gave various concentrations. Our samples gave highest concentration with β-globulin gene. To test if cfDNA may be gene-

selective, it would be interesting to choose several different genes for further investigation. In the literature, Taq-Man probe has been presented as a good method to detect cfDNA as this is a more sensitive than the SYBR green we used [110]. Photometric assay are more suitable for our purposes. Hence, the assay are simple, robust, and with a detection limit of about 1 ng/ml, which is sufficiently sensitive to detect the lowest cfDNA concentration [86].

Our results show that we got slightly higher values with photometric measurement than qRT-PCR. We found the same pattern for plasma samples in qRT-PCR and photometric measurements. Both methods show an increased cfDNA after 30 minutes of reoxygenation.

6.2.3 cfDNA in hypoxia using an animal model

To our knowledge, Tuavea et al [87] are the only publication reporting concentration of cfDNA in the plasma in a premature cohort. However, they used phenol extraction method and quantified with a very basic fluorescence method. Our study is therefore the first study, investigating newborn pigs exposed to hypoxia where cfDNA is measured in different time points after reoxygenation and quantified photometric and with qRT-PCR.

Our hypothesis was that asphyxia-induced ROS has similar pathogenesis as a tumor cells. Thus we expected an increased concentration of cfDNA in neonates with asphyxia. The hypothesis was tested on two different cohorts, which included piglets exposed to various neuroprotective treatments after hypoxia.

The concentration of cfDNA implicates an increased level of cfDNA after 30 minutes of reoxygenation, as detected in figure 5.13 and 5.14, suggesting an increase in oxidative stress. Both cohorts reveal similar patterns. We can confirm that there is an increase in oxidative stress after 30 minutes. On the other hand, literature based on other methods has seen an increased level of cfDNA in cancer patients compared to the control group [91]. Our studies also show that pigs exposed to hypoxia have a higher value of cfDNA compared the control group. The control group shows minimal changes. Decrease in the concentration of cfDNA after 30 minutes might be an effect of the repair mechanisms or cfDNA excretion. Although the difference in the concentrations between the control

group and the intervention groups were no significant, a tendency towards lower cfDNA in the control group was visible.

In cohort 1, NACA was tested as a neuroprotective treatment after hypoxia. NACA showed a trend of lower concentration of cfDNA than pigs treated only with saline after hypoxia. We therefore speculate that NACA could have an impact, but as our study has a limited number of samples, further studies should be conducted to confirm that NACA has an organ protective effect.

Cohort 2 provided hypothermia as a treatment after hypoxia for protective of oxidative damages. Today, hypothermia is one of the few treatments against hypoxia damages. Hypoxia group in this cohort exhibit the same trend as in cohort 1, however hypothermia group shows a lower cfDNA concentration than NACA. The hypothermia treatment started after 30 minutes, and we so a lower concentration of cfDNA after treatment. The increase in cfDNA in hypothermia group in the start could be due to influences of surgery.

CSF is a fluid found in the brain and the spinal channel, and it was interesting to investigate if the concentration was higher than in plasma. In order to test the amount of cfDNA in different body fluids, CSF was selected. Studies have shown a more pronounced damage in brain, and therefore we supposed an increased concentration of cfDNA in CSF. NACA has been shown to be permeable through the BBB and different cell membranes including the mitochondrial membrane [106]. Robert M Anger et al [84] studied cfDNA in CSF in woman during pregnancy, and after delivery. The results showed different concentration of cfDNA for instance in cesarean delivery compared to control.

We examined cfDNA in pigs in cohort 1, receiving NACA after they had been exposed to severe and moderate hypoxia. Thus, the pigs exposed to moderate hypoxia, the concentration of cfDNA was significantly higher for the pigs receiving NACA than those receiving saline. Nevertheless, these is preliminary results and are difficult to explain, and should therefore be confirmed with other methods.

Taken together the results shows that several novel biomarkers for asphyxia will be available in the future. We believe that cfDNA may be used as a non-invasive biomarker, so we can easily collect a blood/urine or CSF sample to see if you have a increased concentration of cfDNA that indicate a higher oxidative stress damage.

7.0 Conclusion and further work

In this study, we tested novel biomarkers to estimate oxidative stress generated by asphyxia damage applying a piglet model. Piglets were exposed to hypoxia-reoxygenation and the increase in mutation rate (RMC method), gene expression changes, and changes in the quantity of cfDNA were explored. For the RMC method, our analysis revealed that the mutation ratio correlated with an increase in the oxidative stress level. In addition to DNA damage, increased levels of expression in oxidative stress were also observed at the RNA and protein level. Further, the investigated antioxidant NACA provided neurodegenerative-protection, against oxidative damage.

Different extraction kits were examined to explore the changes in quantity of cfDNA. Our analysis revealed that Qiagen resulted in the highest yield of cfDNA, and porcine DNA was found to be a reliable standard for measuring cfDNA. Our analysis exhibited a higher concentration of cfDNA in pigs compared to human and adult pigs had lower concentration compared to newborn pigs. cfDNA was measured using both qRT-PCR and photometric techniques, and our results revealed higher concentrations with the latter. We expect cfDNA to be used as a novel biomarker and monitoring tool for neonatal asphyxia damages in future.

Further research on DNA damage by using RMC method will include various neuroprotetive agents and in investigating different tissues. Although we prefer to use *12S* for mtDNA and *p53* for ntDNA digestion and mutation detection, other genes and restriction enzymes may also be explored and might be equally efficacious. On the other hand, further testing of extraction methods for cfDNA, like with magnetic beads, may further optimize yield and reliable results for changes at the cfDNA level. In addition to extraction, concentration of cfDNA may also be tested for different genes in qRT-PCR. Different methods like digital PCR, parallel end sequencing may be tested. Different detection dyes like Pico green can be tested in photometric method. There is also a possible to sequence cfDNA and investigate how frequent the sequence is distributed across the gene. In future there will be a possibility to measure the concentration of cfDNA in newborn babies.

8.0 Reference

1. UNICEF. *The State of the World's Children 2014 In Numbers*. 2015; Available from: http://www.unicef.org/sowc2014/numbers/documents/english/SOWC2014_In Numbers_28 Jan.pdf.
2. (WHO), W.H.O. *World Health statistics* 2010; Available from: http://www.who.int/en/.
3. Solberg, R., *Resuscitation of the newborn.* 2011: p. 9-17, 25-27.
4. Wollen, E.J., *Short - and Long- term effects of supplemental oxygen on transcriptome profiles of the newborn* 2014: p. 13 -16.
5. McGuire, W., *Perinatal asphyxia.* Clinical Evidence, 2007: p. 0320.
6. Ersdal, H.L., et al., *Birth Asphyxia: A Major Cause of Early Neonatal Mortality in a Tanzanian Rural Hospital.* Pediatrics, 2012. **129**(5): p. 1238-1243.
7. Barkovich, A.J. and C.L. Truwit, *Brain damage from perinatal asphyxia: correlation of MR findings with gestational age.* American Journal of Neuroradiology, 1990. **11**(6): p. 1087-96.
8. Hospital, S.C.s. *Birth Asphyxia* 2015; Available from: http://www.seattlechildrens.org/medical-conditions/airway/birth-asphyxia/.
9. Volpe, J.j., *Neurology of the Newborn*. Fifth ed. 2008, Philadelphia, USA: Saunders Elsevier
10. Bhalala, U.S., R.C. Koehler, and S. Kannan, *Neuroinflammation and Neuroimmune Dysregulation after Acute Hypoxic-Ischemic Injury of Developing Brain.* Frontiers in Pediatrics, 2014. **2**: p. 144.
11. Lai, M.-C. and S.-N. Yang, *Perinatal Hypoxic-Ischemic Encephalopathy.* Journal of Biomedicine and Biotechnology, 2011: p. 609813.
12. Gunn, A.J. and L. Bennet, *Fetal hypoxia insults and patterns of brain injury: Insights from animal models.* Clinics in perinatology, 2009. **36**(3): p. 579-593.
13. Perlman, J.M., *Pathogenesis of hypoxic - ischemic brain injury.* Perinatology, 2007. **27**.
14. Almaas, R., *Hypoxia in Human NT2-N Neurons*. 2003. p. 41.
15. Burnsed, J.C., et al., *Hypoxia-ischemia and therapeutic hypothermia in the neonatal mouse brain - a longitudinal study.* PLoS One, 2015. **10**(3): p. e0118889.
16. Shankaran, S., et al., *Childhood Outcomes after Hypothermia for Neonatal Encephalopathy.* The New England journal of medicine, 2012. **366**(22): p. 2085-2092.
17. Benterud, T., *Global HI*. From lecture at OUS.
18. Simon, G.A. and H.I. Maibach, *The pig as an experimental animal model of percutaneous permeation in man: qualitative and quantitative observations--an overview.* Skin pharmacology and applied skin physiology, 2000. **13**(5): p. 229-234.
19. Pond, W.G., et al., *Perinatal ontogeny of brain growth in the domestic pig.* Proc Soc Exp Biol Med, 2000. **223**(1): p. 102-8.
20. Laptook, A., B.S. Stonestreet, and W. Oh, *The effects of different rates of plasmanate infusions upon brain blood flow after asphyxia and hypotension in newborn piglets.* J Pediatr, 1982. **100**(5): p. 791-6.
21. Gleadle, J.a.R., Peter, *Hypoxia.* eLs. John Willey & Sons Ltd, April 2001.
22. Devasagayam, T.P., et al., *Free radicals and antioxidants in human health: current status and future prospects.* J Assoc Physicians India, 2004. **52**: p. 794-804.
23. Kirsti Berg, K.L.J., *Oksygen- Venn eller fiende* 2010.
24. Dröge, W., *Free Radicals in the Physiological Control of Cell Function*. Vol. 82. 2002. 47-95.

25. Pacifici, R.E. and K.J.A. Davies, *Protein, Lipid and DNA Repair Systems in Oxidative Stress: The Free-Radical Theory of Aging Revisited.* Gerontology, 1991. **37**(1-3): p. 166-180.
26. Sharma, P., et al., *Reactive Oxygen Species, Oxidative Damage, and Antioxidative Defense Mechanism in Plants under Stressful Conditions.* Journal of Botany, 2012: p. 26.
27. Halliwell, B., *The basics- What they are and how to evaluate them* Adv. Pharmacol, 1997: p. 38: 3-20.
28. Paravicini, T.M. and R.M. Touyz, *NADPH oxidases, reactive oxygen species, and hypertension: clinical implications and therapeutic possibilities.* Diabetes Care, 2008. **31 Suppl 2**: p. S170-80.
29. Trachootham, D., et al., *Redox Regulation of Cell Survival.* Antioxidants & Redox Signaling, 2008. **10**(8): p. 1343-1374.
30. Reuter, S., et al., *Oxidative stress, inflammation, and cancer: How are they linked?* Free Radical Biology and Medicine, 2010. **49**(11): p. 1603-1616.
31. Winerdal, M., et al., *Long Lasting Local and Systemic Inflammation after Cerebral Hypoxic ischemia in Newborn Mice.* PLoS ONE, 2012. **7**(5): p. e36422.
32. Enzo, *Orgins and Consequences of Oxidative Stress*
33. Dalle-Donne, I., et al., *Biomarkers of Oxidative Damage in Human Disease.* Clinical Chemistry, 2006. **52**(4): p. 601-623.
34. Slupphaug, G., B. Kavli, and H.E. Krokan, *The interacting pathways for prevention and repair of oxidative DNA damage.* Mutat Res, 2003. **531**(1-2): p. 231-51.
35. sejersted, Y., *Neil3 DNA Glycosylase in Maintenance and Repair of the Mammalian Brain.* 2012: p. 13-22,29-31.
36. Donigan, K. and J.B. Sweasy, *Sequence Context Specific Mutagenesis and Base Excision Repair.* Molecular carcinogenesis, 2009. **48**(4): p. 362-368.
37. Hakem, R., *DNA-damage repair; the good, the bad, and the ugly.* Embo j, 2008. **27**(4): p. 589-605.
38. De Bont, R. and N. van Larebeke, *Endogenous DNA damage in humans: a review of quantitative data.* Mutagenesis, 2004. **19**(3): p. 169-85.
39. Dr.Krisztián Kvell, D.J.P., Dr.Miklós Székely, Dr.Márta Balaskó, Dr.Erika Pétervári, Dr.Gyula Bakó, *Molecular and Clinical Basics of Gerontology.* Medical Science 2011.
40. Alam, Z.I., et al., *Oxidative DNA damage in the parkinsonian brain: an apparent selective increase in 8-hydroxyguanine levels in substantia nigra.* J Neurochem, 1997. **69**(3): p. 1196-203.
41. Kovalenko, O.A. and J.H. Santos, *Analysis of oxidative damage by gene-specific quantitative PCR.* Curr Protoc Hum Genet, 2009. **Chapter 19**: p. Unit 19.1.
42. Halliwell, B., *Reactive oxygen species and the central nervous system.* J Neurochem, 1992. **59**(5): p. 1609-23.
43. Strand, J.M., et al., *The distribution of DNA damage is defined by region-specific susceptibility to DNA damage formation rather than repair differences.* DNA Repair (Amst), 2014. **18**: p. 44-51.
44. Zhang, H., et al., *A new approach utilizing real-time qPCR to detect in vitro base excision repair.* DNA Repair (Amst), 2010. **9**(8): p. 898-906.
45. Lord, C.J. and A. Ashworth, *The DNA damage response and cancer therapy.* Nature, 2012. **481**(7381): p. 287-94.
46. Maynard, S., et al., *Base excision repair of oxidative DNA damage and association with cancer and aging.* Carcinogenesis, 2009. **30**(1): p. 2-10.
47. Kaniak-Golik, A. and A. Skoneczna, *Mitochondria-nucleus network for genome stability.* Free Radic Biol Med, 2015. **82**: p. 73-104.
48. Tuppen, H.A., et al., *Mitochondrial DNA mutations and human disease.* Biochim Biophys Acta, 2010(2): p. 113-28.

49. Wiesner, R.J., J.C. Rüegg, and I. Morano, *Counting target molecules by exponential polymerase chain reaction: Copy number of mitochondrial DNA in rat tissues.* Biochemical and Biophysical Research Communications, 1992. **183**(2): p. 553-559.
50. Craig, H.C.J., *mtDNA and Mitochondrial Diseases.* Scitable by nature education, 2008.
51. Chan, D.C., *Mitochondria: Dynamic Organelles in Disease, Aging, and Development.* Cell. **125**(7): p. 1241-1252.
52. Halsne, R., et al., *Lack of the DNA glycosylases MYH and OGG1 in the cancer prone double mutant mouse does not increase mitochondrial DNA mutagenesis.* DNA Repair (Amst), 2012. **11**(3): p. 278-85.
53. Malik, A.N. and A. Czajka, *Is mitochondrial DNA content a potential biomarker of mitochondrial dysfunction?* Mitochondrion, 2013. **13**(5): p. 481-92.
54. Tuppen, H.A., et al., *Mitochondrial DNA mutations and human disease.* Biochim Biophys Acta, 2010. **1797**(2): p. 113-28.
55. Wei Wang, P.O., Ragnhild Skinnes, Ying Esbensen, Magnar Bjørås, Lars Eide *Mitchondrial DNA Intergrity Is Essential for Mitochondrial Maturation During Differentiation of Neural Stem Cells* Stem Cells, 2010. **28**.
56. Murphy, Michael P., *How mitochondria produce reactive oxygen species.* Biochemical Journal, 2009. **417**(Pt 1): p. 1-13.
57. Charles Kunsch, R.M.M., *Oxidative Stress as a Regulator of Gene Expression in the Vasculature* Circulation Research, 1999.
58. Sionov RV, H.I., Haupt Y, *The regulation of p53 Growth Supression*. 2000, Madam Curie Bioscience Database
59. Naga Deepthi CH, V.P.K.A., Rameshbabu and U indirapriyadarshini, *Role of Tumor Suppressor Protein p53 in Apoptosis and Cancer Therapy.* Cancer science & Therapy, 2011.
60. Saha, T., R.K. Kar, and G. Sa, *Structural and sequential context of p53: A review of experimental and theoretical evidence.* Prog Biophys Mol Biol, 2014.
61. Wu, Y., et al., *Activities and response to DNA damage of latent and active sequence-specific DNA binding forms of mouse p53.* Proceedings of the National Academy of Sciences of the United States of America, 1997. **94**(17): p. 8982-8987.
62. Saha, M.N., et al., *Pharmacological activation of the p53 pathway in haematological malignancies.* Journal of Clinical Pathology, 2010. **63**(3): p. 204-209.
63. Meek, L.a., *p53, the gatekeeper of the cell.* BioDiscovery, 2013.
64. Ghanem, M.A., et al., *The prognostic significance of apoptosis-associated proteins BCL-2, BAX and BCL-X in clinical nephroblastoma.* Br J Cancer, 2001. **85**(10): p. 1557-1563.
65. Almaas, R., *Hypoxia in Human NT2- N Neurons.* 2003: p. 21-23.
66. Nechushtan, A., et al., *Conformation of the Bax C-terminus regulates subcellular location and cell death.* The EMBO Journal, 1999. **18**(9): p. 2330-2341.
67. Indran, I.R., et al., *Recent advances in apoptosis, mitochondria and drug resistance in cancer cells.* Biochimica et Biophysica Acta (BBA) - Bioenergetics, 2011(6): p. 735-745.
68. Finucane, D.M., et al., *Bax-induced caspase activation and apoptosis via cytochrome c release from mitochondria is inhibitable by Bcl-xL.* J Biol Chem, 1999. **274**(4): p. 2225-33.
69. Yamabe, K., et al., *Cancer gene therapy using a pro-apoptotic gene, caspase-3.* Gene therapy, 1999. **6**(12): p. 1952-1959.
70. Pawlowski, J. and A.S. Kraft, *Bax-induced apoptotic cell death.* Proceedings of the National Academy of Sciences, 2000. **97**(2): p. 529-531.
71. Zhu, X., et al., *Ziyuglycoside II Inhibits the Growth of Human Breast Carcinoma MDA-MB-435 Cells via Cell Cycle Arrest and Induction of Apoptosis through the Mitochondria Dependent Pathway.* International Journal of Molecular Sciences, 2013. **14**(9): p. 18041-18055.

72. Institute, N.C., *Antioxidants and Cancer Prevention.* National institues of health, 2014.
73. Sies, H., *Oxidative stress: oxidants and antioxidants* Experimental Physiology, 1997. **82**: p. 291-295.
74. Emmanouil, C., *Base Excision Repair Pathways*. DNA Repair - On the Pathways to Fixing DNA Damage and Errors. 2011.
75. BLOKHINA, O., E. VIROLAINEN, and K.V. FAGERSTEDT, *Antioxidants, Oxidative Damage and Oxygen Deprivation Stress: a Review.* Annals of Botany, 2003. **91**(2): p. 179-194.
76. Ates, B., L. Abraham, and N. Ercal, *Antioxidant and free radical scavenging properties of N-acetylcysteine amide (NACA) and comparison with N-acetylcysteine (NAC).* Free Radic Res, 2008. **42**(4): p. 372-7.
77. Sunitha, K., et al., *N-Acetylcysteine amide: a derivative to fulfill the promises of N-Acetylcysteine.* Free Radic Res, 2013. **47**(5): p. 357-67.
78. Price, T.O., et al., *A novel antioxidant N-acetylcysteine amide prevents gp120- and Tat-induced oxidative stress in brain endothelial cells.* Exp Neurol, 2006. **201**(1): p. 193-202.
79. Amer, J., D. Atlas, and E. Fibach, *N-acetylcysteine amide (AD4) attenuates oxidative stress in beta-thalassemia blood cells.* Biochim Biophys Acta, 2008(2): p. 249-55.
80. Goldstein, G.A., *N-acetylcysteine amide (NAC amide) for the treatment of diseases and conditions associated with oxidative stress*. 2013, Google Patents.
81. Wagner, J., *Free DNA--new potential analyte in clinical laboratory diagnostics?* Biochem Med (Zagreb), 2012. **22**(1): p. 24-38.
82. Hashad, D., et al., *Free circulating tumor DNA as a diagnostic marker for breast cancer.* J Clin Lab Anal, 2012. **26**(6): p. 467-72.
83. Gormally, E., et al., *Circulating free DNA in plasma or serum as biomarker of carcinogenesis: Practical aspects and biological significance.* Mutation Research/Reviews in Mutation Research, 2007. **635**(2–3): p. 105-117.
84. Angert, R.M., et al., *Cell-free fetal DNA in the cerebrospinal fluid of women during the peripartum period.* Am J Obstet Gynecol, 2004. **190**(4): p. 1087-90.
85. Jung, K., et al., *Increased cell-free DNA in plasma of patients with metastatic spread in prostate cancer.* Cancer Lett, 2004. **205**(2): p. 173-80.
86. Jung, K., M. Fleischhacker, and A. Rabien, *Cell-free DNA in the blood as a solid tumor biomarker--a critical appraisal of the literature.* Clin Chim Acta, 2010. **411**(21-22): p. 1611-24.
87. Tuaeva, N.O., Z.I. Abramova, and V.V. Sofronov, *The origin of elevated levels of circulating DNA in blood plasma of premature neonates.* Ann N Y Acad Sci, 2008: p. 27-30.
88. Siravegna, G. and A. Bardelli, *Genotyping cell-free tumor DNA in the blood to detect residual disease and drug resistance.* Genome Biology, 2014. **15**(8): p. 449.
89. Elshimali, Y.I., et al., *The Clinical Utilization of Circulating Cell Free DNA (CCFDNA) in Blood of Cancer Patients.* International Journal of Molecular Sciences, 2013. **14**(9): p. 18925-18958.
90. Forshew, T., et al., *Noninvasive identification and monitoring of cancer mutations by targeted deep sequencing of plasma DNA.* Sci Transl Med, 2012. **4**(136): p. 136ra68.
91. Wu, T.L., et al., *Cell-free DNA: measurement in various carcinomas and establishment of normal reference range.* Clin Chim Acta, 2002. **321**(1-2): p. 77-87.
92. Suzuki, N., et al., *Characterization of circulating DNA in healthy human plasma.* Clin Chim Acta, 2008. **387**(1-2): p. 55-8.
93. Day, E., P.H. Dear, and F. McCaughan, *Digital PCR strategies in the development and analysis of molecular biomarkers for personalized medicine.* Methods, 2013. **59**(1): p. 101-107.

94. Szpechcinski, A., et al., *Evaluation of fluorescence-based methods for total vs. amplifiable DNA quantification in plasma of lung cancer patients.* J Physiol Pharmacol, 2008. **59 Suppl 6**: p. 675-81.
95. van der Vaart, M. and P.J. Pretorius, *Is the role of circulating DNA as a biomarker of cancer being prematurely overrated?* Clinical Biochemistry, 2010. **43**(1–2): p. 26-36.
96. Crowley, E., et al., *Liquid biopsy: monitoring cancer-genetics in the blood.* Nat Rev Clin Oncol, 2013. **10**(8): p. 472-484.
97. Anker, P., et al., *Detection of Circulating Tumour DNA in the Blood (Plasma/Serum) of Cancer Patients.* Cancer and Metastasis Reviews, 1999. **18**(1): p. 65-73.
98. Tsui, D.W.Y., R.W.K. Chiu, and Y.M.D. Lo, *Epigenetic approaches for the detection of fetal DNA in maternal plasma.* Chimerism, 2010. **1**(1): p. 30-35.
99. Bianchi, D.W., *From prenatal genomic diagnosis to fetal personalized medicine: progress and challenges.* Nat Med, 2012. **18**(7): p. 1041-1051.
100. Fotakis, G. and J.A. Timbrell, *In vitro cytotoxicity assays: Comparison of LDH, neutral red, MTT and protein assay in hepatoma cell lines following exposure to cadmium chloride.* Toxicology Letters, 2006. **160**(2): p. 171-177.
101. Goldshtein, H., M.J. Hausmann, and A. Douvdevani, *A rapid direct fluorescent assay for cell-free DNA quantification in biological fluids.* Ann Clin Biochem, 2009. **46**(Pt 6): p. 488-94.
102. Tuma, R.S., et al., *Characterization of SYBR Gold nucleic acid gel stain: a dye optimized for use with 300-nm ultraviolet transilluminators.* Anal Biochem, 1999. **268**(2): p. 278-88.
103. Biosoft, P. *PCR Primer Design Guidelines*. 27.04.2015; Available from: http://www.premierbiosoft.com/tech_notes/PCR_Primer_Design.html.
104. Pfaffl, M.W., *Relative quantification.* 2002: p. 63-82.
105. Vermulst, M., J.H. Bielas, and L.A. Loeb, *Quantification of random mutations in the mitochondrial genome.* Methods (San Diego, Calif.), 2008. **46**(4): p. 263-268.
106. Penugonda, S., et al., *Effects of N-acetylcysteine amide (NACA), a novel thiol antioxidant against glutamate-induced cytotoxicity in neuronal cell line PC12.* Brain Res, 2005(2): p. 132-8.
107. Selivanova, G., *Therapeutic targeting of p53 by small molecules.* Semin Cancer Biol, 2010. **20**(1): p. 46-56.
108. Holger Zetzsche, H.-P.K., Michael J. Raupach, Thomas Knebelsberger &Birgit Gemeinholzer, *Comparison of methods and protocols for routine DNA extraction in the DNA Bank Network.* DNA Bank Network, 2012.
109. Day, E., P.H. Dear, and F. McCaughan, *Digital PCR strategies in the development and analysis of molecular biomarkers for personalized medicine.* Methods, 2013. **59**(1): p. 101-7.
110. Chiappetta, C., et al., *Use of a new generation of capillary electrophoresis to quantify circulating free DNA in non-small cell lung cancer.* Clinica Chimica Acta, 2013. **425**(0): p. 93-96.
111. (M.D), J.L., *Intelligent Mitochondria Communication with Neurons.* 2014.
112. al, R.e., *Cancer Epidemiol Biomarkers Prev* 2002.

9.0 Appendix

A. Solutions

Table A.1: **Blotting buffer (5X)**

RIZMA® base	15.15 g
Glycine	72.10 g
Adjust MQ water to total volume	1 L

Table A.2: **Running buffer (10X)**

TRIZMA® base	30.3 g
Glycine	144 g
SDS	10 g
Adjust MQ water to total volume	1 L

Table A.3: **TBS (10X)**

TRIZMA® base	24.23 g
NaCl	80.06 g
Adjust MQ water to total volume	1 L
HCl	Adjust to pH 7.6

Table A.4: **TBS-T**

10X TBS	100 ml
MQ water	900 ml
Tween 20	1 ml

Table A.5: **TBS-T with 5% non-fat dry milk**

Non-fat dry milk	1.5g
1X TBS-T	30 ml

Table A.6: **MTT solution**

MTT	0.025 g
Glucose	550 µM
PBS	50 ml

Table A.7: **TAE buffer (10 X)**

Tris base	48.4 g
Glacial acetic acid (17.4M)	11.4 ml
EDTA, disodium salt	3.7 g
Adjust MQ water to total volume	1 L

Table A.8: **Agarose gel (3%)**

MetaPhor Agarose	3 g
1 X TAE	100 ml
Gelred	10 µl

B. Genomic information

For RMC method were genes selected based on the highly mutated gene area. For mtDNA *12S* loci was chosen, while for ntDNA p53 was chosen.

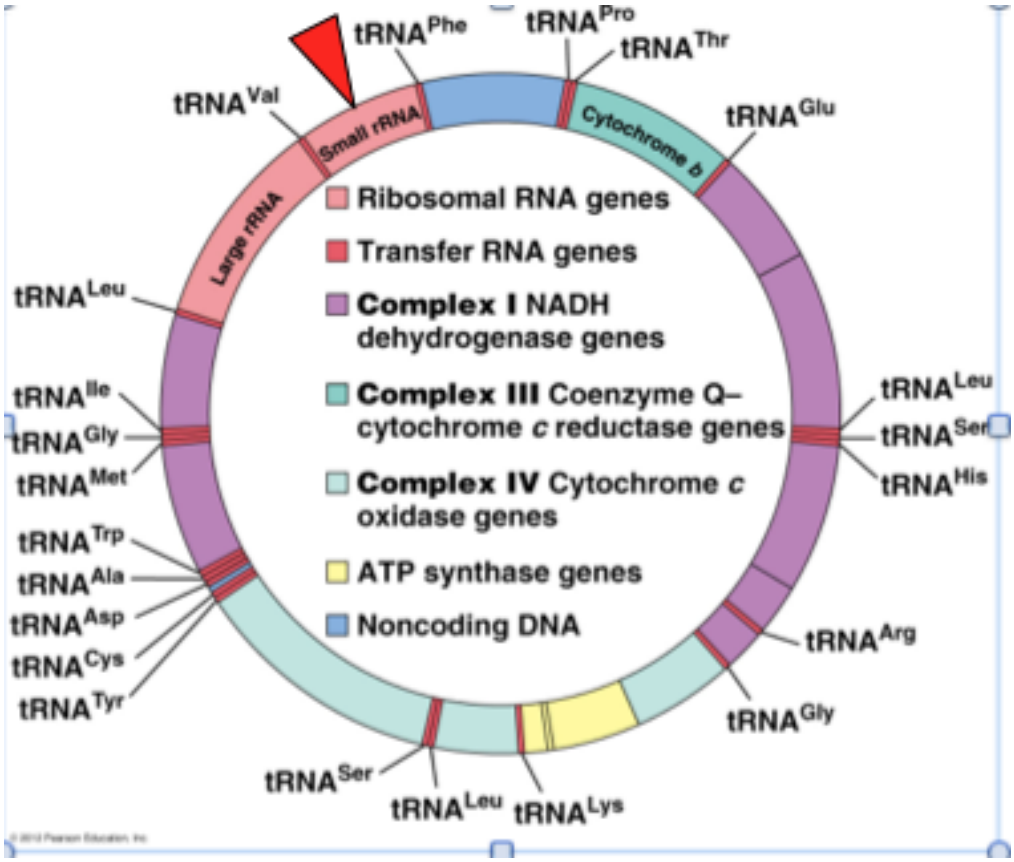

Figure 9.1: mtDNA at *12S* loci. The red arrow shows where our restriction site is placed in the loci [111].

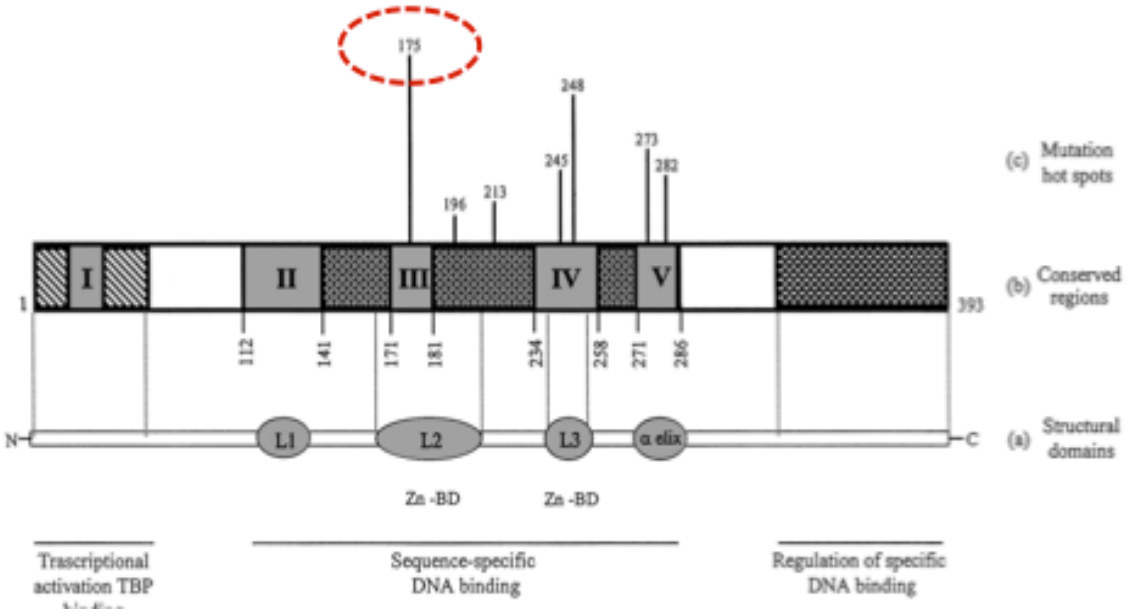

Figure 9.2: ntDNA at p53 gene, the mutation site 175 was chosen to investigate with RMC method [112].

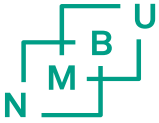

Norwegian University
of Life Sciences

Postboks 5003
NO-1432 Ås, Norway
+47 67 23 00 00
www.nmbu.no